KINETIC STUDY OF SELECTIVE CO OXIDATION ON Au / Al_2O_3 CATALYST

by

Mehtap Demir

B. S. in Ch.E., Yıldız Technical University, 2006

Submitted to the Institute for Graduate Studies in
Science and Engineering in partial fulfillment of
the requirements for the degree of
Master of Science

Graduate Program in Chemical Engineering

Boğaziçi University

2009

to my family

ACKNOWLEDGEMENTS

Firstly, I would like to express my sincere thanks to my thesis supervisor, Assoc. Prof. Ramazan Yıldırım for the direct supervision of my work and his patience. I am grateful to his guidelines and helpful comments.

I would like to express my great appreciations to my thesis committee members, Prof. Zeynep İlsen Önsan and Assoc. Prof. Hasan Bedir, who spent their time to read and comment on my thesis.

I would like to thank to Tuğba Davran Candan for her friendship and spending her time to teach me what I need to know for my thesis. Special thanks to Fatma Akpınar, Seval Özdemir, Funda Dikman and Melek Selcen Başar for giving me their friendship, and to Arman Basmacıoğlu for his computational aid and his friendship. Their friendship and support has given me strength.

Cordial thanks for Bilgi Dedeoğlu, Nurettin Bektaş and Yakup Bal for their technical assistance and help.

Finally, I wish to thank my family for their continuous support all these years in any possible way. Without them, I would not achieve anything and there are not enough words, which can describe my love.

Financial support provided by the Boğaziçi University Research Fund through project BAP08A501D and by the Scientific and Technical Research Council of Turkey through project 105M034 is gratefully acknowledged. Besides, I appreciatively acknowledge the graduate scholarship provided by TÜBİTAK MÜNİR BİRSEL FOUNDATION.

ABSTRACT

KINETIC STUDY OF SELECTIVE CO OXIDATION ON Au/Al_2O_3 CATALYST

Kinetic study of selective CO oxidation was performed over Au/Al_2O_3 catalyst prepared using homogeneous deposition-precipitation method. First, the alternative models proposed for the similar catalytic systems in the literature were examined, and the reaction rate equations in terms of elementary reactions were built. Only the single-site mechanisms proceeding on Au surface were considered since the Al_2O_3 support is belived to be inert for CO oxidation. It was also assumed that the presence of H_2, H_2O and CO_2 in the feed stream affected the rate parameter, but not the reaction mechanism. The rates of CO consumption were evaluated in a microflow reactor operating in differential mode using ten set of CO and O_2 concentrations both in the absence and presence of 10 per cent H_2O and 25 per cent CO_2 for two residence times at the temperatures ranging from 90°C to 130°C. The kinetic parameters were estimated using experimental data for all plausible mechanisms proposed. Finally, the model discrimination was performed for the most plausible models using the experimentally measured and calculated data. The monofunctional mechanism based on the adsorption of O_2 and CO on the gold sites seems to represent the experimental data best. Finally, the effects of temperature on the rate of CO consumption was investigated using simplified one-site and power law models at temperatures ranging 90°C to 130°C both in the absence and presence of H_2O and CO_2, and the activation energies were calculated using Arrhenius plot.

ÖZET

Au/Al_2O_3 KATALİZÖRÜ ÜZERİNDE SEÇİMLİ KARBON MONOKSİT OKSİDASYONUN KİNETİK ÇALIŞMASI

Homojen tortu çöktürmesi yöntemi ile hazırlanmış Au/Al_2O_3 katalizörü üzerinde seçimli karbon monoksit oksidasyonun kinetik çalışması gerçekleştirilmiştir. İlk olarak, literatürde benzer katalitik sistemler için öngörülen modeler incelenmiş ve elementer reaksiyonlara dayalı reaksiyon hız denklemleri kurulmuştur. Al_2O_3 destek malzemesi inert olduğu için sadece Au üzerinde tek merkez üzerinde gerçekleşen CO oksidasyon mekanizmaları üzerinde durulmuştur. Besleme akımında varolan hydrogen, su buharı ve karbon dioksitin hız parametrelerini etkilediği ama bu bileşenlerin reaksiyon mekanizmalarını etkilemedikleri kabul edimiştir. Karbon monoksit tüketim hızları differansiyel rejimde çalışan bir mikroakış reaktörü içinde on farklı karbon monoksit ve oksijen konsantrasyonu kullanılarak hem yüzde 10 su buharı ve yüzde 25 karbon monoksit varlığında hem de su buharı ve karbon monoksitin yokluğunda iki farlı kalma süresinde ve 90-130°C sıcaklık aralığında elde edilmiştir. Kinetik parametreler önerilen bütün makul mekanizmalar için deneysel veriler kullanılarak hesaplanmıştır. Son olarak, en makul modeller arasından deneysel olarak ölçülen veriler ile hesaplanan veriler kullanılarak model ayrımı gerçekleştirilmiştir. Altın üzerinde O_2 ve CO adsorpsiyonuna dayanan tek merkezli mekanizmanın deneysel sonuçları en iyi temsil ettiği gözlenmiştir. Bunlara ek olarak, sıcaklığın karbon monoksit tüketim hızı üzerindeki etkileri 90-130°C sıcaklıkları arasında hem su buharı ve karbon monoksit varlığında hem de yokluğunda güç kanunu modeli ve basitleştirilmiş tek merkezli model kullanılarak araştırılmış, her iki model için de aktivasyon enerjileri Arrhenius grafiği kullanılarak hesaplanmıştır.

TABLE OF CONTENTS

LIST OF FIGURES

LIST OF TABLES

LIST OF SYMBOLS/ABBREVIATIONS

F_{CO}	CO flow
k_{-i}	Rate constant of backward reaction of step I
K_i	Rate constant of forward reaction of step I
K_i	Equilibrium constant of reaction step I
r_{CO}	Reaction rate of CO
R^2	Regression coefficient
ν_{max}	Maximum velocity
W_{CAT}	Weight of catalyst
X_{CO}	CO conversion
ΔH°	Enthalpy of the reaction at the standart conditions
θ_{CO}	Equilibrium CO coverage
θ_{CO_2}	Equilibrium CO_2 coverage
θ_O *	Coverage of adsorbed oxygen on gold sites
AFC	Alkaline Fuel Cell
ATR	Autothermal Reforming
DP	Deposition-Precipitation
FTIR	Fourier Transform Infrared
HDP	Homogeneous Deposition-Precipitation
HPLC	High Performance Liquid Chromatography
HTS	High Temperature Shift
LTS	Low Temperature Shift
MCFC	Molten Carbonate Fuel Cell
MEA	Membrane Electrod Assembly
M-M	Michaelis-Menten
NMRO	Noble Metal Reducible Oxide
PAFC	Phosphoric Acid Fuel Cell
PEMFC	Proton Exchange Membrane Fuel Cell

PEM	Polymer Electrolyte Membrane
PROX	Preferential Oxidation
SOFC	Solid Oxide Fuel Cell
SR	Steam Reforming
STS	Scanning Tunneling Spectroscopy
WGS	Water-Gas Shift Reaction

1. INTRODUCTION

Due to increasing population and growth in economy, the demand for energy is becoming higher and is expected to increase 1.5 to 3 times by 2050 (Liu and Zhang, 2008). Environmental Literacy Council estimated that, in 2005, over 85 per cent of our energy demands are met by the combustion of fossil fuels which are related to environmental damage such as global climate change and air pollution.

One of the most promising alternatives for various applications ranging from small-scale portable devices to stationary power generation and automobiles is fuel cell technology, which is less polluting and can be two to three times more efficient than internal combustion engine in converting fuel to electricity (Mhadeshwar and Vlachos, 2005). A variety of fuel cells have already been developed, but the proton exchange membrane fuel cells (PEMFC) are being actively tested for fuel cell cars, buses and trucks. Pure hydrogen acts as the fuel in PEMFCs with the advantage of simple system integration and high efficiency, but the major problem in the widespread commercialization is insufficient infrastructure for hydrogen storage and transportation (Kim and Lim, 2002). Hence on board generation of H_2 from natural gas, gasoline or other hydrocarbons becomes an attractive alternative (Önsan, 2007).

Recently, the production of hydrogen is investigated and employed in three processes; a) steam reforming, b) partial oxidation, and c) autothermal reforming (Ersoz *et. al.*, 2006). In these processes, the resulting gas mixture contains significant amounts of CO and it is further processed in a water-gas shift (WGS) reactor where gas mixture becomes richer in H_2 (Avgouropoulos *et. al*., 2002). However, the hydrogen stream from a fuel processor typically contains 0.5-1.0 per cent CO which must be removed (Günay and Yıldırım, 2008). Eliminating CO from the hydrogen feed is an essential issue for good operation of PEMFCs, since CO at concentrations higher than 10 ppm poisons the anode catalyst (Pansare *et. al*., 2005).

There are many available methods for CO removal such as methanation, Pd-based membranes and selective CO oxidation. Among them, selective CO oxidation seems to be the most effective because of its relatively simple implementation, lower operating costs

and minimal hydrogen loss (Avcı *et. al*., 2001). Compared to the selective CO oxidation, Pd-based membrane needs high pressure difference and fairly high temperature to diffuse hydrogen through membrane, and methanation has more hydrogen consumption (3 molecules of hydrogen per molecule of carbon monoxide) (Holladay *et. al*., 2004).

The catalysts proposed for selective CO oxidation include noble metal catalysts (Pt, Ru, Rh) and base-metal oxides (Cu, Ni, Co), which must be very active and selective for the oxidation of CO, and inactive for the undesired oxidation of H_2 in the temperature range 80-200°C (Caputo *et. al*., 2008). However, supported noble catalysts exhibit an optimum in CO conversion and selectivity to CO_2 at higher temperatures. The CO oxidation, on the other hand, is rather slow due to inhibition of oxygen adsorption by adsorbed CO at lower temperatures (Grisel and Nieuwenhuys, 2001b).

Gold based catalysts have received wide attention ever since Haruta *et. al.* found that gold nanoparticles on metal oxides exhibit higher catalytic activity and better selectivity towards CO_2 formation in CO oxidation than platinum and copper at low temperatures (Iizuka *et. al*., 2009). Additionally, lower prices than platinum make the gold more attractive for fuel cell applications (Yu *et. al*., 2007). The nature and the structure of the support play a vital role in determining the activity of gold catalysts (Menegazzo *et. al*., 2009).

Kinetics and mechanisms for CO oxidation reaction on the supported gold catalyst still remain uncertain (Aguilar-Guerrero and Gates, 2008). The metal-support interaction (interface effect), the presence of low-coordinated atoms on the nanoparticles (geometry effect) and the low dimensionality of the gold structures are all significant in a reaction to elucidate the mechanism of CO oxidation on Au (Azar *et. al*., 2006).

Reaction kinetics is based on elementary steps, such as CO and O_2 adsorption, desorption and surface bonding that explain how the overall reaction proceeds. To date it is difficult to bring the synergy of the connection between elementary reactions and their consequences on the rate of overall CO oxidation reaction over gold (Wojciechowski and Asprey, 2000). Modeling via elementary steps allows adapting the kinetic model when the

catalyst formulation is changed in order to introduce new catalytic functions (Hoebink *et. al*., 2001).

The Au/Al_2O_3 catalyst used in this study was first prepared and the effects of calcinations and reduction environments over 1 per cent Au/Al_2O_3 catalyst were investigated by Tezcanlı (2008). Additionally, the promotional effects of ceria, cobalt, nickel, magnesium, manganese and iron were studied, and $Au/MgO/Al_2O_3$ showed a good catalytic activity for CO oxidation in the presence of H_2O and CO_2.

In this study, kinetics of selective CO oxidation in hydrogen-rich stream over Au/Al_2O_3 catalyst prepared by homogeneous deposition precipitation method was performed. Temperature programmed reaction technique was used in order to examine the effects of concentrations of CO and O_2 on the CO conversion and reaction rate in the temperatures between 90-130°C. First of all, rate expressions were estimated from possible CO oxidation mechanisms proposed in the literature. Then the rate calculations were performed with various feed compositions in the absence and the presence of H_2O and CO_2, and the kinetic parameters were obtained and the model discrimination was performed. Additionally, the temperature effect on reaction rate was studied.

The study consists of five chapters. Chapter 2 focuses on a literature survey involving fuel cells, hydrogen production methods and preferential CO oxidation with criteria for the selection of catalysts used. The reaction mechanisms for CO oxidation and kinetic analysis methods are also described in Chapter 2. Chapter 3 indicates the experimental work with catalyst preparation procedures and conditions for kinetic measurements. Results and discussion are presented in Chapter 4. Conclusions from this study and recommendations for future work are dealt with in Chapter 5.

2. LITERATURE SURVEY

The lack of sustainability of the current energy system and environmental impact of fossil fuels are motivating efforts to develop and adopt alternative energy models. One of these is what is known as the hydrogen economy, based on the use of hydrogen as a carrier of the energy generated from renewable sources. Hydrogen and fuel cell technologies are seen as a key solution for 21st century energy problem.

2.1. Fuel Cell

Fuel cell technology is a recent interest in generating electricity for various applications because of high energy efficiency and environmentally friendly nature (Lee *et. al*., 2008). For systems designed to consume hydrogen directly, the only products are electricity, water and heat.

Welsh scientist Sir William Robert Grove, demonstrated the first fuel cell in 1839, discovered that by arranging two platinum electrodes with one end of each immersed in a container of sulfuric acid and the other ends separately sealed in containers of oxygen and hydrogen, a constant current would flow between the electrodes. The sealed containers held water as well as the gases, and he noted that the water level rose in both tubes as the current flowed. By combining several sets of these electrodes in a series curcuit, he created what he called a "gas battery".

A fuel cell consists of an electrolyte layer in contact with a porous anode and cathode on either side. In a typical fuel cell, fuel, commonly hydrogen, is fed continuously to the anode (negative electrode) and an oxidant, often oxygen from air, is fed continuously to the cathode (positive electrode). The two electrodes of a fuel cell are separated by an ion- conducting electrolyte. On the anode side, hydrogen from the bulk difuses through the anode where it later dissociates into H^+ ions and electrons by a catalytic reaction. On the cathode side, oxide ion is formed by reduction with the electrons available (Jayasankar *et. al*., 2009). Electrons return from the electrical circuit that performs work on load while the ions migrate through the electrolyte toward oppositely charged electrode, where ions combine to form water (Song, 2002).

2.1.1 . Types of Fuel Cell

A variety of fuel cells are in different stages of development. The major types of fuel cells, as defined by both the type of the electrolyte and the temperature of operation, are the proton exchange membrane fuel cell (PEMFC), the alkaline fuel cell (AFC), the phosphoric acid fuel cell (PAFC), the molten carbonate fuel cell (MCFC) and the solid oxide polymer fuel cell (SOFC) (Alcaide *et. al*., 2006).

MCFC and SOFC operate at high temperatures (600-1200°C). High temperature fuel cells have the higher fuel flexibility, the lowest fuel-quality demands and furthermore high temperature limits damage from carbon monoxide poisoning since CO is directly oxidized electrochemically (Seitarides *et. al*., 2008). However, high operating temperature is associated with problems like requirement for high performance of materials, sealing problems caused by thermal expansion and difficulties in thermal management (Yang *et. al*., 2009). AFC, PEMFC and PAFC, on the other hand, operate at low temperatures (<200°C). Low temperature fuel cells have minimal corrosion problems and quick start-up. However, these fuel cells extremely sensitive towards impurities, therefore the anode catalyst, mainly platinum, is strongly poisoned by CO.

Among these types of fuel cells, PEMFC has been attracting much attention in the application to electric vehicles or residential power-generations because of high efficiency, quick start-up capability with lower operating temperature, high power density (Lai *et. al.*, 2008).

The PEM consists of a perfluorinated polymer backbone with sulfonic acid side chains. The membrane, two layers of catalyst (platinum supported on carbon particle), and two gas diffusion electrodes are assembled into a membrane electrode assembly (MEA) (Yu *et. al*., 2009). To function, the membrane must conduct hydrogen ions (protons) but not electrons as this would in effect short circuit the fuel cell. The hydrogen rich fuel is delivered to the anode side of the MEA. At the anode side it is catalytically split into protons and electrons (Reaction 2.1). The protons permate through the PEM to the cathode side. The electrons travel along an external load circuit to the cathode side of the MEA.

The oxygen in the cathode gas stream is delivered to the cathode side of the MEA where it reacts with the protons and electrones to form water molecules (Reaction 2.2).

$$\text{Anode reaction: } 2H_2 \rightarrow 4H^+ + 4e^- \quad (2.1)$$

$$\text{Cathode reaction: } O_2 + 4H^+ + 4e^- \rightarrow 2H_2O \quad (2.2)$$

Pure hydrogen is an ideal fuel for PEMFCs. However, poor storage capacity, safety problems and lack of the infrastructure associated with hydrogen use are potentially major disadvantages. Furthermore, amounts of CO (>10 ppm) in the H_2 fuel can poison the fuel-cell catalyst. Thus, on board and demand production of hydrogen is possibly an attractive approach to the problems. In H_2 production system, several reactions are involved: hydrocarbon fuel oxidation state, water-gas shift (WGS), preferential oxidation (PROX) (Georgaka *et. al*., 2008).

2.2. On Board Hydrogen Production Methods for Fuel Cell

In order to both economically competitive and environmental concerns, hydrogen as an energy carrier can be produced from steam reforming (Reaction 2.3), partial oxidation (Reaction 2.4), and auto-thermal reforming (Reaction 2.5) using decarbonized fossil and petroleum-based fuels such as natural gas, which is mainly methane, LPG, gasoline, diesel, methanol and ethanol (Önsan, 2007; Holladay *et. al*., 2009). The choice of hydrogen production method is based on the type of fuel cell, the demands and volume of the systems, and heat management strategy (Ghenciu, 2002).

Steam Reforming Reaction:

$$\text{SR: Fuel} + \text{Steam} \rightarrow \text{Carbon oxides} + \text{Hydrogen} \qquad \Delta H_r > 0 \quad (2.3)$$

Partial Oxidation Reaction:

$$\text{POX: Fuel} + \text{Air} \rightarrow \text{Carbon oxides} + \text{Hydrogen} + \text{Nitrogen} \qquad \Delta H_r < 0 \quad (2.4)$$

Auto-thermal Reforming Reaction:

$$\text{ATR: Fuel} + \text{Steam} + \text{Air} \rightarrow \text{Carbon oxides} + \text{Hydrogen} + \text{Nitrogen} \quad \Delta H_r \leq 0 \qquad (2.5)$$

Steam reforming is advantageous for large-scale hydrogen production since maximum hydrogen efficiency and low carbon monoxide content is possible. However, steam reforming is an endothermic process and energy demand must be supplied to the reformer, usually transferred into the system from outside (Rabenstein and Hacker, 2008).

Compared to steam reforming, start-up time and start-up energy demand should be as low as possible for both partial oxidation and autothermal reforming due to exothermic processes (Rabenstein and Hacker, 2008). Partial oxidation is fast reaction therefore this process offers the advantage of smaller reactors and higher throughputs (Ghenciu, 2002). The autothermal reforming combines the thermal effects of partial oxidation and steam reforming in an single unit. With less fuel energy wasted at start-up, this system is accepted to be more energy efficient to produce hydrogen (Adachi *et. al*., 2009). During the three processes, carbon monoxide is produced. The production of carbon monoxide, a poison to the fuel cell electrocatalysts, needs to be avoided. To reduce the amount of carbon monoxide, the reformer is followed by water-gas-shift reactor in fuel processing systems (Sandoval *et. al*., 2007).

2.3. Water-Gas-Shift Reaction

The water gas shift (WGS) is a key reaction in the production of hydrogen for a number of processes. The exit product coming out of the SR-based reformer containing up to 12 per cent CO and that of the ATR-based reformer containing 6-8 per cent CO is passed into WGS reactors, where CO is reacted with water to form CO_2 and hydrogen, given in Reaction (2.6) (Önsan, 2007). This reaction is important because it not only reduces the amount of CO, but also produces additional hydrogen (Leppelt *et. al*., 2006).

$$CO + H_2O \Leftrightarrow H_2 + CO_2 \qquad \Delta H = -41.1 \text{ kJ/mole} \qquad (2.6)$$

WGS reaction is midly exothermic and thermodynamic equilibrium controlled; hence, it is favoured at low temperature. However, kinetically, the catalysts are not active to attain the equilibrium at low temperatures and the fast reaction kinetics can be achieved at high temperatures (Pradhan *et. al*., 2009). The operating temperature furhermore affects the CO concentrations in the product gas. Obviously temperature is considered to be an important control factor for WGS processes (Trimm, 2005).

Generally WGS reaction is carried out in two stages; a high temperature shift (HTS) unit and low temperature shift (LTS) unit coupled with a cooling system to get the hot gases to cool down to optimum reaction temperatures (Haryanto *et. al*., 2007). The exit stream from the high temperature WGS reactor operating at 300-450°C contains 3-4 per cent CO which is further reduced to 0.5-1 per cent after the gases pass through the low temperature WGS reactor operating at 200-300°C (Trimm, 2005; Önsan, 2007). In industrial applications, Fe-Cr oxide catalysts are used for the HTS reaction, while the LTS catalysts commonly used are $Cu/ZnO/Al_2O_3$ or precious metal-based catalysts. However the existing WGS catalysts are sensitive to air and suffer from low activity (Natesakhawat *et. al*., 2006).

2.4. Preferential CO Oxidation in H_2-Rich Streams

Palladium-based membrane purification, catalytic CO methanation, and preferential CO oxidation (PROX) are effective methods of CO clean up down to 10-50 ppm from the reformate stream before entering the fuel cell. One obvious route is to diffuse hydrogen through a Pd-based membrane, can be simplified because the control system to the heat and the air injection rate required in the PROX system is not necessary (Park *et. al*., 2009). However, the membrane system requires high pressure and temperature. The other effective method of removal CO is catalytic CO methanation, where methanation reactors are simpler in that no air is required; however, a large amount of H_2 is consumed for every CO reacted, compared with PROX. Additionally, the method requires careful control of the reactor conditions to be maintained in order to minimize unnecessary consumption of the hydrogen because the carbon dioxide reacts with hydrogen (Holladay *et. al*., 2009). As a result, the preferential CO oxidation is the most promising way to reduce CO to the desired

level due to the low process cost, moderate operating temperature and atmospheric pressure operation (Hwang *et. al*., 2009).

- Preferential CO oxidation

$$CO + 0.5\ O_2 \rightarrow CO_2 \qquad \Delta H_{298} = -283.0\ kJ/mol \quad \text{(desired reaction)} \tag{2.7}$$

$$H_2 + 0.5\ O_2 \rightarrow H_2O \qquad \Delta H_{298} = -242.0\ kJ/mol \quad \text{(undesired reaction)} \tag{2.8}$$

- Methanation

$$CO + 3\ H_2 \rightarrow CH_4 + H_2O \qquad \Delta H_{298} = -283.6\ kJ/mol \tag{2.9}$$

- Water-gas shift

$$CO + H_2O \rightarrow CO_2 + H_2 \qquad \Delta H_{298} = -41.1\ kJ/mol \tag{2.10}$$

In the PROX reaction system, there are two main competing reactions; CO oxidation, where CO is oxidized by O_2 in H_2-rich reformed gas, given in Reaction (2.7), and H_2 oxidation, where H_2 is competitively oxidized by O_2 in Reaction (2.8). H_2 oxidation is undesired reaction; thus, it is important to minimize this reaction to improve the efficiency of the PROX (Yu *et. al.,* 2007). Two possible side reactions can also occur in PROX reaction system; water-gas shift, given in Reaction (2.10) and methane formation from CO in Reaction (2.9). WGS reaction is not harmful, since it reduces the amount of CO present. Nevertheless, the methanation reaction should be avoided because it consumes large amount of hydrogen, reducing the total efficiency.

In order to achieve the low CO concentration (10 ppm), the PROX reactor is placed between the low-temperature WGS (~200°C) and the PEMFC (~80°C). Hence, it should operate between low temperatures (Son *et. al*.,2002).

2.5. Catalysts for Selective CO Oxidation at Low Temperatures

Generally, conventional catalysts are not active at low temperatures and have low O_2/CO ratios since oxygen and carbon monoxide competes for the same sites. Under these conditions, carbon monoxide is dominantly adsorbed on the metal surface; hence, carbon monoxide adsorption prevents oxygen adsorption and surface reaction. On the other hand, oxygen is adsorbed too strongly to be displayed by carbon monoxide over base-metal oxide catalysts at low temperatures. Thus, the suitable catalyst should adsorb carbon monoxide, provides activated oxygen, while hydrogen adsorption must be surppressed for the effective CO oxidation (Trimm and Önsan, 2001).

The reformate containing mostly hydrogen, its oxidation leads to a decrease in the overall fuel efficiency because water produced through hydrogen oxidation may affect catalyst activity. Thus, the catalyst for CO oxidation has to selectively oxidize carbon monoxide without oxidizing any of the present 30-70 per cent hydrogen. The lower the selectivity of the process, the higher the required ratio O_2/CO has to be in order to completely oxidize CO to CO_2. However, the excess O_2 also increases hydrogen losses by undesired oxidation (Oliva *et. al*., 2008).

Judging from these requirements, effective PROX catalysts should ideally exhibit both high CO oxidation activity at low temperatures and high selectivity with respect to the side oxidation reaction of H_2. Such catalysts should also tolerate the presence of CO_2 and H_2O (Chen *et. al*., 2008).

Recently, possible catalysts based on either supported noble metals or base-metal oxides are used for the selective oxidation of CO. Noble metals such as platinum, palladium, ruthenium and gold exhibit high activity and selectivity at low temperatures, however; due to their high cost and sensitivity to sulfur poisoning, base-metal catalysts such as copper/copper oxide deserve more attention for lower cost and their activities similar to that of noble metal catalysts (Li *et. al*., 2007).

Metal oxide catalysts contain both transition metal and its oxide such as copper/copper oxide, silver/silver oxide, nickel/nickel oxide, and the higher and lower

oxides of cerium (Park *et. al*., 2009). The most investigated alternative system to noble metals for selective CO oxidation is CuO supported on CeO_2. Martinez-Arias *et. al.* (2006) claimed that the facile redox interplay between copper and cerium is the key factor of high performances of CuO/CeO_2 catalysts for preferential oxidation of CO in H_2-rich streams.

Gurbani *et. al*. (2009) determined the effects of the preparation methods on the performance of the catalyst for the selective oxidation of CO. Two 7 wt.% $CuO\text{-}CeO_2$ catalysts were prepared using wet impregnation method and deposition-precipitation (DP) method. The study showed that the catalyst prepared by DP exhibited a lower capacity to release the lattice oxygen to form CO_2.

In general, the noble metals are supported on reducible transition metal oxides, mainly on SnO_2, MnO_x, Fe_2O_3, CeO_x, CoO_x or on inert oxides such as Al_2O_3, SiO_2 and MgO (Daniells *et. al.,* 2005). The noble metal reducible oxide (NMRO) catalysts have very important applications mostly involving oxidation or reduction reactions where transfer of oxygen atoms takes place. These catalysts exhibit a strong synergy between the two metal components producing significantly higher catalytic activities. The noble metal and the reducible oxide alone can not catalyze CO oxidation at low temperatures (<100°C); hence, low-temperature NMRO catalysts must exhibit strong metal-support interaction (Trimm and Önsan, 2001).

Among noble metal catalysts, platinum catalysts are by far the most extensively studied catalysts. Supported platinum catalysts usually show a high CO conversion at high temperatures (150-250°C) but the catalytic activity decreases at low temperatures (<100°C). Because PEMFC is usually operated below 200°C, the catalysts operating at low temperatures can be more plausible. To increase catalytic activity and selectivity at low temperatures, different methods are tried for supported platinum catalysts such as adding promoters (Fe, Ce, Co), sol-gel preparation, water pretreatment or using reducible oxides as supports (CeO_2, ZrO_2, TiO_2) (Souzo *et. al.,* 2007).

Due to the effects of support on activity of catalyst, some authors in particular have examined the influence of the support in selective CO oxidation on Pt catalysts. Souzo *et. al*. (2007) inspected the Pt catalysts supported over alumina, silica, zirconia and ceria in

total (H_2-free streams) and selective (H_2-rich streams) oxidation of CO. According to their study, the catalysts supported over ceria and zirconia showed higher activity than alumina and silica supported catalysts at low temperatures, but with lower CO conversions.

Ince *et. al.* (2005) investigated the effects of reaction temperature and feed composition on CO conversion and selectivity using 1.4 wt.% Pt-1.25 wt.% Co-1.25 wt.% Ce/Al_2O_3. In this study, the 100 per cent CO conversion was achieved at 90°C, whereas O_2 conversion was about 55-60 per cent at the same temperature (corresponding to 40-45 per cent selectivity toward CO oxidation). The effect of O_2/CO ratio was also investigated and the results showed that the 1 per cent CO can be completely removed using 1 per cent O_2 at 90°C without CO_2 and H_2O.

The kinetics and mechanism of the selective CO oxidation over Pt supported catalysts have been examined extensively. Özyönüm *et. al.* (2007) studied kinetics of low temperature CO oxidation in hydrogen-rich streams with realistic gas compositions over Pt-Co-Ce/Al_2O_3 catalyst and then obtained kinetic parameters in the initial rate region using 8 different sets of CO and O_2 concentrations at 110°C. Baltacıoğlu *et. al*. (2007) investigated CO and O_2 dependency of CO oxidation rate and the effect of the presence of H_2 in the feed using 1 wt.% Pt-0.25 wt.% SnO_x supported on HNO_3-oxidized activated carbon. According to their study, CO oxidation rate negatively depended on CO and positively depended on O_2.

2.5.1. Gold Based Catalysts in H_2-Rich Streams

Gold as noble metal has long been considered to be chemically inert and catalytically inactive as a catalyst because of its poor chemisorption of the bulk state. However, since the work of Haruta's group in the late 1980s, supported gold nanoparticles are well-known for their ability to catalyze CO oxidation in the low temperature range (Wen *et. al*., 2008). Gold catalysts have also lower cost than platinum catalysts and highly selectivity towards CO oxidation. For catalysts in selective CO oxidation, high activity and selectivity towards CO_2 formation are two important characteristics; hence, the interest in these catalysts has continuously increased for this reaction at typical fuel cell operating temperatures (Pansare *et. al*., 2005).

Gold (Au), placed in Group 11 of the periodic table, has an electronic structure of $4f^{14}5d^{10}6s^{1}$. Copper is in the same group and platinum is in Group 10 in the same row. The catalytic activity is associated with the position in the periodic table or energetic parameters. The chemical and physical properties of gold differ from those of the elements in Group 11, but some of its physical properties are similar to those of platinum (Bond *et. al*., 2006). However, gold has the highest electronegative and high oxidation potential. Before Haruta illustrated the catalytic oxidation of CO by the nano-sized gold particles on metal oxide at -73°C, gold used to considered to be inactive because its electrons are not easily transferred (Tseng *et. al.,* 2008).

Since the discovery that supported gold cataysts are very active in low temperatures, three main areas have been studied; (i) understanding the nature of the active sites and reaction mechanism of gold nanoclusters, (ii) optimization of the catalyst structure/composition and (iii) testing the gold catalysts in a series of other catalytic reactions. In spite of the extensive research in these areas, answer to questions is still not known for sure (Centeno *et. al*., 2006).

The particle size, support materials and preparation methods are important factors for creating a good gold catalyst. The catalytic activity can be dramatically affected by the gold nanoparticle size. When gold particle size is reduced to the nanometer range, Au loses its nobleness and shows reactive properties (Prestianni *et. al*., 2009). Much higher activities are shown by oxide-supported small gold particles less than about 5 nm in size. The fact about the gold particle size has initiated a search both for an explanation of this quite unexpected effect and for chemical reactions that are catalyzed by Au (Hvolbaek *et. al*., 2007). Haruta and Date (2001) investigated the effect of the Au particle sizes on the catalytic performance, focusing on Au/TiO_2 together with the effect of preparation conditions and pretreatments. It was concluded that smaller Au particles increased catalytic activity for CO oxidation.

The preparation method is another important property for catalytic activity. The nature of the Au precursors, the method to introduce Au to the support (e.g. co-precipitation, deposition, precipitation, impregnation) and the pH affect particle size, the particle shape and the amount of residual chloride (which can poison a Au/Al_2O_3 catalyst)

in the catalyst. Luengnaruemitchai *et. al*. (2004) studied the effect of preparation method on the catalytic activity of Au/CeO_2 in the presence of H_2 over the temperature range of 50-190°C and it was found that Au/CeO_2 prepared with co-precipitation exhibited the highest activities. Khoudiakov *et. al.* (2005) compared two Au/Fe_2O_3 catalysts prepared by deposition-precipitation and conventional coprecipitation, with the same amount of gold precursor. According to their study, the deposition-precipitation technique produced more active catalysts because of more complete precipitation of the gold from solution.

Tests performed by Soares *et. al*. (2003) on CO oxidation using an Au/TiO_2 catalyst prepared by impregnation and deposition precipitation give data showing non-catalytic and catalytic behaviour. In this study, the conversion of CO appeared to be very high, but it was difficult to distinguish whether it was catalytic or non-catalytic reacted. Perhaps the active types of oxygen can be reabsorbed for the deposition precipitation catalyst, making it active at room temperature. Active oxygen cannot apparently be reabsorbed on incipient wetness catalysts in a significant amount, probably due to loss of surface area and poisining by Cl^- ions. Concluding, the catalyst prepared by DP is much more active in low temperature CO oxidation. Results are shown at least two ways in with CO can be oxidized by gold;

- through reaction of surface active oxygen species activated by gold during the preparation of the catalysts.
- through catalytic reaction mediated by gold.

The pretreatment of the catalyst such as calcination affects the gold loading and the catalytic activity for selective CO oxidation (Chang *et. al*., 2009). Gold has low melting temperature, that could provoke gold particle sintering during calcination. Therefore the calcination temperature is important for the particle size during preparation. At too high temperature an increase in the gold particle size and a decrease in the catalytic activity are observed. Addition to calcination temperature, the presence of chloride is responsible for gold particle growth during calcination; hence, a washing treatment is applied in order to remove chloride from the gold catalyst (Ivanova *et. al*.,2006b).

Among these factors, catalyst support is usually considered crucial to determining the catalytic activity. The selection of the support material depends on the reaction that is performed: (a) supports as a source of oxygen for the reaction are active in reaction, such as TiO_2, ZrO_2, CeO_2, and (b) supports are inert in reaction, such as Al_2O_3, SiO_2, MgO (Ribeiro *et. al.,* 2008). Highly dispersed gold particles supported on reducible and catalytically active supports exhibit synergetic behaviour with gold (Quinet *et. al*., 2008b). The effect of the support on the oxidation of CO over gold catalyst was investigated by Ivanova *et. al.* (2006a). According to this study, both inert and active supports were tested in the CO oxidation reaction and it was concluded that gold catalysts supported on reducible type metal oxides are generally more active. Interestingly, unsupported gold, on the other hand, exhibits a higher activity in the H_2 oxidation than in the low- temperature CO oxidation (Haruta, 2004). The fact that supported gold is more active in CO oxidation provides the unique ability to put together a highly reactive and selective catalyst for CO oxidation in the presence of H_2 (Grisel *et. al*., 2002).

Rossignol *et. al.* (2005) discussed support effects in the selective CO oxidation in the presence of H_2 by using Au/Al_2O_3, Au/ZrO_2, and Au/TiO_2 catalysts. According to the study, it was found that the influence of H_2 on the CO conversion depended on the support; hence, the reactivity for CO oxidation was presented in the following order; Au/Al_2O_3< Au/ZrO_2< Au/TiO_2.

Romero-Sarria *et. al*.(2008) studied the role of water in the CO oxidation on a metallic monolith coated with 1 per cent Au/CeO_2 catalyst. It is concluded that the presence of water provokes a modification of the catalyst properties when temperature increases. However, the activities in the presence and absence of water are similar at temperature lower than 80°C.

The reduction program and the cooling atmosphere after reduction are important for catalytic activity. Szabo *et. al*.(2007) changed the atmosphere of cooling from an inert gas to hydrogen after reduction in hydrogen at 350°C using Au/MgO and Au/Al_2O_3 catalysts. This study showed that the extend of cooling effect depends on the amount of gold in these catalysts.

Chang *et. al*.(2007) observed the study on Au/CeO_2 and Au/MnO_2 catalysts for CO oxidation at low temperature using X-ray diffraction, transmission electron microscopy, and X-ray photoelectron spectroscopy in order to analyze the structure, morphology, and electronic properties of the catalysts. In this study, Au^0 and Au^{3+} were obtained on Au/CeO_2 catalysts, while only metallic gold was detected on Au/MnO_2. Au/CeO_2 exhibited higher activity than Au/MnO_2 toward CO oxidation.

2.5.2. Aluminum Oxide (Al_2O_3) Support

Al_2O_3 is considered as the most preferable support in industrial catalytic process. Despite less active as compared with other metal oxides, the active alumina is a good model system because of its simplicity and activity at higher temperatures than 27°C (Venkov *et. al*., 2006).

Among support materials, TiO_2 is currently the best support for gold nanoparticles in the catalytic oxidation of CO. However, CO conversion on Au/Al_2O_3 is higher than other supported gold catalysts at low temperatures in the presence of H_2 because of dissociative adsorption of oxygen. Actually, at low temperatures all supported gold catalysts exhibit high selectivity for CO_2. Oxidation of H_2 affects the activities of the catalysts in the presence of H_2, but the Au/Al_2O_3 catalyst is the least affected. (Rossignol *et. al*., 2005). Quinet *et. al*. (2008a) presented the hydrogen effect in the low temperature PROX reaction over a 0.9 per cent Au/Al_2O_3 catalyst and carried out kinetic study in the range 20-280°C. They showed that CO oxidation rate is significantly increased at low temperature in the presence of a small amount of hydrogen in the reactant gas mixture. The selectivity for CO_2, on the other hand, declined drastically at higher temperatures because of the oxidation of H_2.

H_2O plays an important role in generating active supported gold catalysts, the exact nature of this role, however, is not yet understood. Therefore, the role hydroxyls in the mechanism of CO oxidation has received greater attention. Date *et. al*. (2007) reported the enhancing effects of H_2O in the $CO+O_2$ stream for calcined samples of Au/TiO_2 and Au/Al_2O_3. They proposed a twofold role for the moisture; one was the activation of the

oxygen from the support, and the second was the decomposition of the carbonate intermediate.

Zou *et. al.* (2007) investigated the activity and the deactivation of Au/Al_2O_3 catalyst for low-temperature CO oxidation. The activity of the catalyst was changed after separate treatment in the following different atmosphere: (i) O_2+N_2+CO, (ii) O_2+N_2 heated above 100°C and (iii) $O_2+N_2+H_2O$ vapor. In the first atmosphere, because of the accumulation of carbonate-like species on the catalyst surface, the deactivation by CO occured. The treatment showed that the addition of H_2O vapor in the atmosphere inhibited the deactivation effectively. When the catalyst was treated at the higher temperatures, the activity of the catalyst decreased seriously and the removal of OH groups at active sites during heating caused the deactivation by thermal treatment. The activity of the catalyst treated by air with H_2O vapor decreased with increasing the concentration of H_2O vapor. The treatment indicated that the growth of gold particle size was responsible for the activity decrease of the catalyst.

Transition metal oxides as a promoter has two effects on Au/Al_2O_3 catalyst. Addition of MO_x (M=Mg, Mn, Fe, Co, Ni, Cu and Zn) may prevent small Au particles on Al_2O_3 from sintering in heat treatments up to 700°C; hence, the active sites on the catalyst can be stabilized. Another effect of MOx on Au/Al_2O_3 is to increase the catalytic activity. The activity of the H_2 oxidation decreases under the operating conditions of PEMFCs because high CO conversion is achieved on $Au/MOx/Al_2O_3$ (Grisel *et. al*., 2002). Grisel and Nieuwenhuys (2001a) investigated the effects of addition of transition metal oxides on low temperature CO oxidation over Au/Al_2O_3. The activity of $Au/MOx/Al_2O_3$ can be concluded in the following order: $MnO_x>NiO_x>ZnO_x>FeO_x>CoO_x>CrO_x>CuO_x$.

A comparative study of two gold-containing catalysts, Au/Al_2O_3 and $Au/CeO_2/Al_2O_3$ prepared by deposition-precipitation, reported by Centeno *et. al*.(2006). In this work, the $Au/CeO_2/Al_2O_3$ sample exhibited a much higher catalytic activity in the CO oxidation reaction due to the higher dispersion of gold on CeO_2/Al_2O_3 as compared to Al_2O_3 and a strong promoting effect of ceria in the oxidation of the Au^0 sites for CO adsorption. In addition, it was concluded that isolated Au^+ sites were more active in CO oxidation than metallic gold particles.

Grisel *et. al*. (2002) elucidated the second promoter effect on $Au/MgO/Al_2O_3$ catalyst in the presence of 70 vol.% H_2 at the temperatures relevant to hydrogen fuel cell applications. On the basis of their results addition of MnO_x and FeO_x to $Au/MgO/Al_2O_3$ improved CO oxidation activity especially at low temperatures. CO conversion generally increased with increasing O_2/CO ratio but CO_2 selectivity decreased. The $Au/MnO_x/MgO/Al_2O_3$ catalyst exhibited the highest activity when O_2/CO ratio was 2 or 4 and the best result was for $Au/FeO_x/MgO/Al_2O_3$ catalyst at the ratio 4.

Mozer *et. al*. (2009) investigated the effect of Cu addition on Au/Al_2O_3 used in the selective oxidation of CO in the presence of H_2. The addition of 0.5 and 1 wt.% of copper to 2.5 per cent Au/Al_2O_3 enhanced the CO conversion at low temperature because of an interaction between Au and Cu on the surface of the catalyst. Additionally, the O_2 content was varied from 0.5 to 1.5 per cent, while the CO concentration was kept constant (1%). The result was that the CO/O_2 ratio equal to 1 demostrated higher CO conversion.

2.6. Kinetics of CO Oxidation over Supported Gold Catalysts

The interest in catalysis and kinetics is still important in homogeneous and heterogeneous reactions for industrial applications. During the past century most industrial processes were resolved, but there is a lack of developments of catalysts and processes in environment, fuel cells, natural gas conversion, new materials and nowadays in biotechnology (Schmal *et. al*., 2005). Kinetics and mechanism for reactions on the catalyst, and its involvement in the reaction, are still not known for sure since catalytic reactions on solid surfaces have great complexity (Khan and Albano, 2002).

2.6.1. Surface Reaction for CO Oxidation

The reaction between CO and activated oxygen may take place on the support or on the gold particles. Many authors assume that CO is adsorbed on metallic gold sites and, mainly at higher CO partial pressure, also at the border between metallic gold particles and the support. In spite of the extensive research on CO oxidation catalyzed by supported gold, the mechanism of the reaction and the nature of its active sites yet remain unclear (Aguilar-Guerrero and Gates, 2008).

2.6.1.1. Electronic Transition Structure: There can exist a transition state between the electronic structure and behaviour of bulk gold, and that of discrete gold atoms. This transitional state could exhibit activity towards other species, whereas the bulk does not.

In order to investigate a possible correlation between the electronic properties and the specific activity of the Au clusters in more detailed, scanning tunneling spectroscopy (STS) measurements were carried out on a Au/TiO_2 (110) catalyst by Lai *et. al*. (1998). Data were acquired by recording topographic images of individual nanometer sized Au clusters, and simultaneously investigating its electronic properties. It was obvious that a metal to non-metal transition occurs as the cluster size approaches approximately 4 nm in diameter, corresponding to the size at which catalytic activity begins for CO oxidation.

It is concluded that the activity of the catalyst is determined by the unique electronic structure of its Au clusters. A maximum in the catalytic activity with respect to the mean diameter of the Au clusters is observed where the transition of the electronic state of the specific Au cluster occurred from metallic to non-metallic. This structure influences the adsorption energy of CO on gold.

2.6.1.2. Presence of Ionic Au Species: Although metallic Au appears to be indispensable, a question arises as to why the periphery of Au particles can activate O_2 molecules at low temperatures. As discussed by Kung *et. al*. (2003), it is probable that the perimeter interfaces contain oxidic Au species under usual conditions wherever H_2O is present at concentrations above 1 ppm. A chemical model that involves an ensemble of metallic Au atoms and Au cations with hydroxyl ligands has been suggested (Figure 2.1.). It is assumed that the Au cation can remain sufficiently stable in a reducing environment and in the neighborhood of metallic gold. It seems more likely that Au(I) would be able to satisfy these requirements than Au(III). Therefore, Au(I)-OH has been proposed as the cationic Au component.

There appears to be increasing support that the active site involves the perimeter of the Au particles or the Au support interface and for the presence of Au cations in the active catalysts although their role in the reaction is not yet accepted unequivocally. In the

literature it is stressed that presence of ionic gold species alone is not sufficient for activity, metallic gold particles are needed at all times.

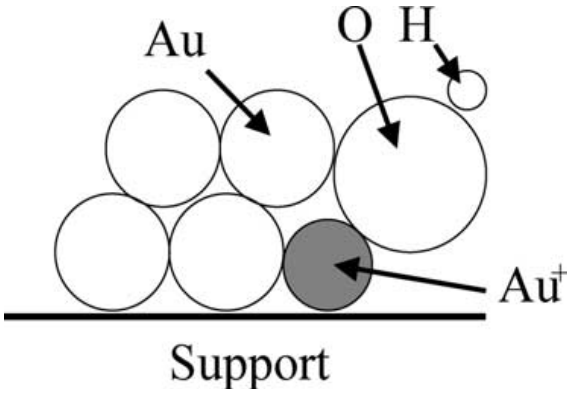

Figure 2.1. Model of the active Au(I)-OH site for CO oxidation (Kung *et.al*., 2003)

2.6.1.3. Specific Surface Site: Specific sites may be present at the surface. It is known that CO binds considerably stronger to stepped surfaces than on flat (111) terraces. Lopez *et. al.* (2004) observed that the chemical activity of gold is strongly dependent on the coordination number of the gold atoms and the strength of the Au–CO and Au–O bond varies strongly with the Au coordination number. They found that the Au atoms in the surface of an Au(111) have d states that are so low in energy that they are unable to interact strongly with the O 2p valence states. This gives a weak bond-so weak that O bonds stronger to another O atom than to the Au(111) surface, and O_2 does not dissociate on Au(111).

The need for a stepped surface to facilitate chemical activity is in accordance with behaviour seen for other catalytically active metal surfaces. Since the relative concentration steps and other surface defects increases with decreasing particle size. On top of that, the important fine tuning provided by different supports is given by a range of effects, most of which are related to defects in the support. These effects also explain why reducible supports generally give more active catalysts that nonreducible one.

2.6.1.4. Electronic Interaction Between Au and Support: An electronic interaction between the gold and the support may occur. Manzoli *et. al*. (2003) performed a Fourier transform infrared (FTIR) study at low temperature on nanosized gold dispersed on ZrO_2 and on

TiO_2. Both the supports had the same gold particle sizes, but CO and O_2 adsorption and interactions evidenced some differences between the two samples. Zirconia is a large gap insulating oxide, while titania is an n-type semiconducter, containing an excess of anionic vacancies (Boccuzzi *et. al*., 2000). According to Manzoli *et. al*. (2003), the changes by adsorption can be effective, influencing the chemical properties of gold surface sites, while the large gap on Au/ZrO_2 makes difficult any electronic interaction between gold and zirconia.

2.6.2. Reaction Mechanisms for CO Oxidation over Supported Gold Catalysts

It is possible to understand the large range in reaction rates in terms of the reaction mechanisms and the nature of elementary processes. Since the classical steps of a catalytic reaction (e.g. adsorption, surface reaction, desorption) do not proceed at the same rate, reaction mechanism is based upon elementary steps. Elementary step modelling is a model that can be determined experimentally for one global reaction. It is sometimes argued that elementary step kinetics contain so many parameters that any description of experimental data. Each step preferably is proven relevant on the basis of experimental evidence, and quite often such relevance has already been reported in the literature from studies that applied completely different techniques (Hoebink *et al.,* 2001).

It is generally accepted that the mechanism of the low-temperature CO oxidation occurs on Au via a two-step mechanism, given in Reaction (2.11) and (2.12);

$$CO + O_2 \rightarrow CO_2 + O \qquad \text{(slow reaction)} \tag{2.11}$$

$$CO + O \rightarrow CO_2 \qquad \text{(fast reaction)} \tag{2.12}$$

The catalytic activity on Au catalyst is high at lower temperatures, compared to what is observed on Pt and other transition metals, for the following two reasons (Gavril *et. al*., 2007);

a) The easy dissociation of O_2 on Pt at low temperature greatly reduces the possibility of CO+O_2 on Pt and other transition metals.

b) CO oxidation through the CO+O reaction, after the dissociation of O_2, possesses an intrinsically high barrier on Pt compared to that on Au. The mild bonding character is accepted as the basis of the catalytic properties of Au.

In some cases the mechanism of CO oxidation reaction can be explained by a simple Langmuir-Hinshelwood mechanism for non-competitive adsorption, combined with an additional mechanism of oxygen activation. This reaction comprises the following elementary steps in Table 2.1, where "*"denotes an adsorption site on Au surface.

Table 2.1. Langmuir-Hinshelwood mechanism for CO oxidation over an Au catalyst (Gottfried and Christmann, 2004)

Elementary Step	Step Number
$CO + * \underset{k_{d,CO}}{\overset{k_{a,CO}}{\Leftrightarrow}} CO*$	(1)
$O_2 + * \underset{k_{d,O_2}}{\overset{k_{a,O_2}}{\Leftrightarrow}} O_2*$	(2)
$O_2* + * \underset{k_{rec,O}}{\overset{k_{diss,O_2}}{\Leftrightarrow}} 2O*$	(3)
$CO* + O* \overset{k_r}{\rightarrow} CO_2* + *$	(4)
$CO_2* \overset{k_{d,CO_2}}{\rightarrow} CO_2 + *$	(5)

In the mechanism by gold catalyst using this model, O_2 is assumed to be directly adsorbed on Au particles and oxygen atoms are formed by the breaking of O-O bonds. On gold sites, oxygen atoms react with CO to yield CO_2.

However, in other cases Langmuir-Hinshelwood model is not particularly good for CO oxidation over supported Au catalysts (Long *et. al*., 2008). Therefore, various mechanistic models have been developed.

It is uncertain whether the oxygen molecule is dissociatively or non-dissociatively adsorbed (Liu *et al*., 2002), but most likely molecular oxygen is adsorbed at the perimeter interface. The perimeter interfaces appear to be the most reasonable to account for the whole characteristic behaviour of nanoparticulate Au catalysts. The interfaces can explain the increase in side steps on Au surfaces as the sites for CO adsorption and the ideas for support surfaces as the sites for O_2 adsorption. The adsorbed O_2 can move to the step, edge and corner sites of Au nanoparticules, but more probably, it reacts with CO adsorbed on the Au surfaces at the perimeter interfaces (Haruta, 2004).

Boccuzzi *et. al*. (2001) suggested two different pathways for CO oxidation over supported Au catalysts. First, O_2 activated on the surface of metallic gold particles reacts directly and rapidly with CO. The proposed OC-Au-Ox intermediate decompeses to yield CO_2. Second, O_2 activates CO, or CO adsorbed at the border of Au support interface reacts with surface lattice O_2 from the support, results mainly in carbonates. They proposed that the former mechanism appears to be more relevant for the high activity in low-temperature CO oxidation.

The kinetic findings indicate that hydrogen apparently enhances the CO oxidation rate before hydrogen starts to be oxidized. Several authors have showed that the presence of hydrogen in feed stream allows to reduce and even prevent deactivation of many gold catalysts at low temperature. Costello *et. al.* (2003) proposed that hydrogen inhibits the formation of formate and carbonate species (formed from reaction of CO with the surface hydroxycarbonyl species) which are thought to be poisons for the CO oxidation.

In the presence of both O_2 and H_2, highly active –OOH species are formed on the surface of the Au catalyst, presented in Table 2.2., where "*" denotes an adsorption site on Au surface. Therefore, surface Au atoms are covered with these –OOH species, even before the catalyst is ramped to 280°C. At low temperatures, CO would be oxidized using these –OOH surface species and H_2 should be the limiting reactant, the oxidation of CO being directly related to the amount of –OOH formed from H_2 (Quinet *et. al*., 2008a). Although the above proposed mechanism based on the presence of H_2 contributes to the mechanism of CO oxidation, its contribution is not expected to be important in the mechanism (Georgaka *et. al*., 2008).

Table 2.2. Mechanism of the formation of H_2O from O_2 and H_2 over Au/Al_2O_3 catalyst in the presence of H_2 (Quinet *et. al*., 2008a)

Elementary Step	Step Number
$H_2 + 2* \overset{k_{11}}{\rightarrow} 2H*$	(1)
$O_2 + * \overset{k_2}{\rightarrow} O_2*$	(2)
$O_2* + H* \underset{k_{-3}}{\overset{k_3}{\Leftrightarrow}} OOH* + *$	(3)
$OOH* + H_2 + * \underset{k_{-4}}{\overset{k_4}{\Leftrightarrow}} H_2O_2* + *$	(4)
$H_2O_2* + * \underset{k_{-5}}{\overset{k_5}{\Leftrightarrow}} 2OH*$	(5)
$OH* + H* \underset{k_{-6}}{\overset{k_6}{\Leftrightarrow}} H_2O* + *$	(6)

The mechanism of CO oxidation over supported Au catalyst is suggested by Haruta, Kung and Bond. The three mechanisms all proceed via bidentate carbonate formation, but the reaction and adsorption sites differ.

2.6.2.1. The Mechanism Proposed by Bond: Bond and Thompson (2000) proposed the following mechanism, involving Au-hydroxide groups.

It is suggested that the mechanism starts by a support hydroxyl ion attacking a CO molecule on the Au, step (3) in Table 2.3. It is thought this may occur more generally, and propose a periphery mechanism as follows. The Au^0-CO is attacked by an hydroxyl group either on a support cation or on a peripheral Au^{III} ion, forming a carboxylate group attached to the latter. This is in turn attacked by a superoxide, which must be responsible for oxidizing two carboxylate ions: the hydroxyl group returns and is ready to re-engage in the catalytic cycle, step (6) in Table 2.3., where "Au" denotes an adsorption site on Au surface and"$*_{sup}$" denotes an adsorption site on the support surface.

Table 2.3. The mechanism of CO oxidation over supported Au catalyst (Bond and Thompson, 2000)

Elementary Step	Step Number
$Au^0 + CO \xrightarrow{k_1} Au^0\text{-}CO$	(1)
$Au^{III} + OH^-_{sup} \xrightarrow{k_2} Au^{II}\text{-}OH$	(2)
$Au^0\text{-}CO + Au^{II}\text{-}OH \xrightarrow{k_3} Au^{II}\text{-}COOH + Au^0$	(3)
$O_2 + *_{sup} + e^- \underset{k_{-4}}{\overset{k_4}{\Leftrightarrow}} O_2^- *_{sup}$	(4)
$Au^{II}\text{-}COOH + O_2^- *_{sup} \xrightarrow{k_5} Au^{II} + CO_2 + HO_2^- *_{sup}$	(5)
$Au^{II}\text{-}COOH + HO_2^- *_{sup} \xrightarrow{k_6} Au^{II} + CO_2 + 2HO^-_{sup} + *_{sup}$	(6)
$Au^{II} + *_{sup} \xrightarrow{k_7} Au^{III} + *_{sup} + e^-$	(7)

2.6.2.2. The Mechanism Proposed by Haruta: Haruta showed that three temperature regions exist where different rates and apparent activation energies. Based on the study, Haruta and Date (2001) postulated a model in which bidentate carbonates adsorbed on the support are important intermediates for CO_2 formation.

As seen in Table 2.4., where "Au" denotes an adsorption site on Au surface and"sup" denotes an adsorption site on the support surface, the reaction takes place only at step, edge and corner sites on the Au particles with almost 0 kJ/mol for apparent activation energy at temperatures below -73°C. The reaction cannot proceed on the support or at the perimeter interface between Au and the support because they are covered with carbonate species produced by surface reactions between CO and the support. The catalytic activity can be detected at any temperature when Au particles are small enough. Actually unsupported Au powder (30 nm in diameter) exhibits measurable activity for CO oxidation at -73°C with apparent activation energy of nearly zero.

Table 2.4. The mechanism of CO oxidation over Au/TiO_2 (Haruta and Date, 2001)

Reaction at the Au surface at below -73°C	
Elementary Step	Step Number
$2CO + 2Au(s^a) \underset{k_{-1}}{\overset{k_1}{\Leftrightarrow}} 2Au(s)\text{-}CO$	(1)
$O_2 + Au(s) \overset{k_2}{\rightarrow} Au(s)\text{-}O_2$	(2)
$Au(s)\text{-}CO + Au(s)\text{-}O_2 \overset{k_3}{\rightarrow} CO_2 + Au(s) + Au(s)\text{-}O$	(3)
$Au(s)\text{-}CO + Au(s)\text{-}O \overset{k_4}{\rightarrow} CO_2 + 2Au(s)$	(4)
$Au(p^b)\text{-}CO + Au(p)\text{-}O_2 \overset{k_5}{\rightarrow} CO_2 + Au(p) + Au(p)\text{-}O$	(5)
$Au(p)\text{-}CO + Au(p)\text{-}O \overset{k_6}{\rightarrow} CO_2 + 2Au(p)$	(6)
Reaction at the perimeter interfaces at above 27°C	
$O_2 + sup(p) \overset{k_7}{\rightarrow} sup(p)\text{-}O_2$	(7)
$Au(p)\text{-}CO + sup(p)\text{-}O_2 \overset{k_8}{\rightarrow} CO_2 + Au(p) + sup(p)\text{-}O$	(8)
$Au(p)\text{-}CO + sup(p)\text{-}O \overset{k_9}{\rightarrow} CO_2 + Au(p) + sup(p)$	(9)
Reaction at the perimeter interfaces at below 27°C	
$Au(p)\text{-}CO + sup(p)\text{-}O_2 \overset{k_{10}}{\rightarrow} Au(p) + sup(p)\text{-}CO_3$	(10)
$sup(p)\text{-}CO_3 \overset{k_{11}}{\rightarrow} CO_2 + sup(p)\text{-}O$	(11)

[a]step, [b]perimeter

At temperature above 27°C, the reaction proceeds at the perimeter interfaces between CO adsorbed on the surfaces of Au particles and molecular oxygen adsorbed at the support surface with an activation energy of nearly zero. However, the reaction proceeds much faster by more than one order of magnitude than the reaction over the Au surfaces.

Between -73°C and 27°C, the reaction proceeds at the perimeter interface which is partly covered with carbonate species. The coverage of the species may change depending on temperature, thus giving rise to apparent activation energy around 30 kJ/mol.

2.6.2.3. The Mechanism Proposed by Kung: Kung *et. al*. (2003) proposed a model based on the assumption that reactive ionic Au species are presented in Figure 2.2.

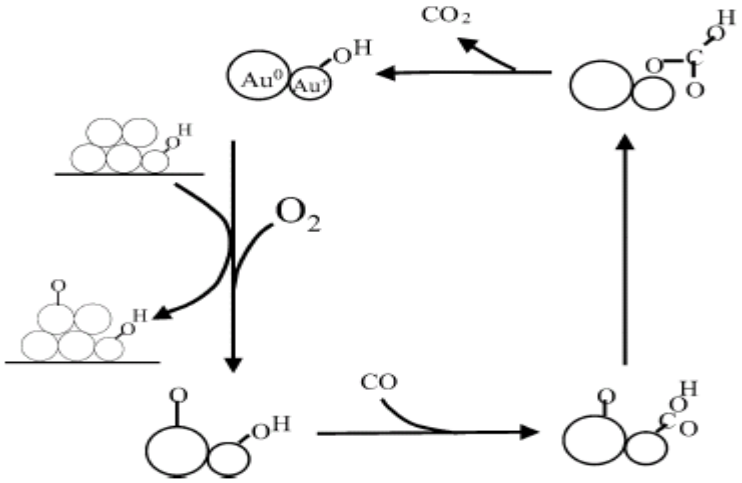

Figure 2.2 Mechanism of CO oxidation on Au/Al_2O_3 catalyst (Kung *et.al*., 2003)

In the mechanism, CO is adsorbed on the Au cation and is inserted into the hydroxyl group to form a hydroxycarbonyl. Stable hydroxycarbonly complexes of many group VIII metals have been prepared and their formation from the CO and OH^- ligands is enhanced by lower electron density at the metal ion. Oxidation of the hydroxycarbonyl will result in the formation of the bicarbonate which is decarboxylated to CO_2, and the active site Au-OH is regenerated.

2.7. Methods of Kinetic Analysis

For kinetic measurements, the ideal tubular reactor, which is called the plug flow reactor, is generally used on heterogeneous catalytic reactions. In this reactors, specific assumptions are made for determining rate equations (Fogler, 2006);

(i) no mixing in the axial direction, i.e. the direction of flow

(ii) no radial gradients in temperature and concentration

(iii) no dispersion

In order to minimize heat transfer resistance at outside and inside walls, determining the rate equation is possible only on the basis of isothermal data. The only remaining possibility is to dilute the catalyst bed unless isothermicity is still achieved. However, since all the fluid streamlines should hit the same number of catalyst particles, excessive dilution should be avoided as well.

To date, it is possible to measure the rate as a function of concentration using differential method and integral method.

In differential method, the amount of the catalyst is relatively small so that the conversion is limited (Froment and Bischoff, 1990). However, the use of the plug flow reactors in these method at low levels of conversion shows significant problems such as high pressure drop due to the required high flow rates (Wojciechowski and Rice, 2003).

The flow rate through the catalyst bed is monitored, as are the entering and exiting concentrations. Therefore, if the weight of the catalyst, ΔW, is known, the rate of reaction per unit mass of catalyst, r_A, can be calculated from the measured conversion, given in Equation (2.13). The continuity equation for A then becomes (Froment and Bischoff, 1990);

$$F_{Ao}\Delta x_A = r_A \Delta W \tag{2.13}$$

In the differential method, the rate equation is directly measured; therefore, the form of the rate equation does not require any assumptions. Additionally, it is much easier to fit to a rate equation. Nevertheless, this method needs many runs (10-100 times longer than integral method); hence, it is useful only when a high degree of accuracy is needed (Masel, 2001).

Due to the difficulties of operating differential method, plug flow reactors are generally operated in an integral way. By varying the ratio W/F_{Ao}, a wide range of

conversion (x) may be obtained. In order to determine the reaction rate, the conversion versus W/F_{Ao} data pertaining to the same temperature have to be differentiated, presented in Equation (2.14), as can be seen from the continuity equation for the reference component A in this type of reactor (Froment and Bischoff, 1990);

$$F_{Ao}dx_A = r_A dW \tag{2.14}$$

and over the whole reactor;

$$\frac{W}{F_{A_0}} = \int_{x_{A1}}^{x_{A2}} \frac{dx_A}{r_A} \tag{2.15}$$

Generally, integral methods require easier experiments than do differential methods, but rate equations are less acurate. The methods are also suitable for all reactions including very fast or very slow ones (Masel, 2001).

3. EXPERIMENTAL WORK

3.1. Materials

3.1.1. Chemicals

The chemicals used for catalyst preparation are listed in Table 3.1.

Table 3.1. Chemicals used in catalyst preparation

Chemicals	Formula	Grade	Source	Molecular Weight (g $mole^{-1}$)
Gold(III) chloride trihydrate	$HAuCl_4.3H_2O$	Extra Pure	Aldrich	393.83
Aluminium oxide	Al_2O_3	Extra Pure	Zeochm EU	101.96
Urea	$CO(NH_2)_2$	Extra Pure	Merck	60.06

3.1.2. Gases and Liquids

All of gases and liquids in kinetic measurements are listed with their applications and specifications in the Table 3.2. and the Table 3.3. Oxygen, carbon dioxide, hydrogen and helium were supplied by Bileşik Oksijen Sanayi (BOS) and carbon monoxide was supplied by HABAŞ Company.

Table 3.2. Applications and specifications of the gases used in the kinetic measurements

Gas	Application	Specification
Carbon monoxide	Reactant, MS calibration	99.0% HABAŞ
Oxygen	Reactant, MS calibration	99.99% BOS
Carbon dioxide	Reactant, MS calibration	99.99% BOS
Hydrogen	Reactant, Reducing agent, MS calibration	99.99% BOS
Helium	Reactant (Inert), MS calibration	99.99% BOS

Table 3.3. Applications and specifications of the liquids used in the kinetic measurements

Liquid	Application	Specification
Water	Reactant, cleaning	Distilled

3.2. Experimental Set-Up

The experimental set-up is composed of a catalyst preparation system, a microreactor flow system, and an analysis system. In the catalyst preparation system, Au was deposited on the γ-Al_2O_3 supports by homogeneous deposition precipitation (HDP) method, studied for selective CO oxidation reaction in our laboratory by Tezcanlı (2008).

The kinetic activities of the catalysts were tested in a microreactor flow system which consists of mass flow controllers for inlet gases, a liquid pump, temperature controller and a fixed bed flow reactor in a furnace. In the analysis system, the feed and product gas streams were analyzed by using mass spectrometer which is connected to the microreactor flow system.

3.2.1. Catalyst Preparation System

Au was deposited on the γ-Al_2O_3 supports by HDP method including a stirrer to achieve homogeneous mixing, a heater circulation bath for controlling the temperature of the HDP method, a pH meter for determination of the alkalinity of the solution and a beaker. A simplified scheme of a preparation system used in HDP process is presented in Figure 3.1.

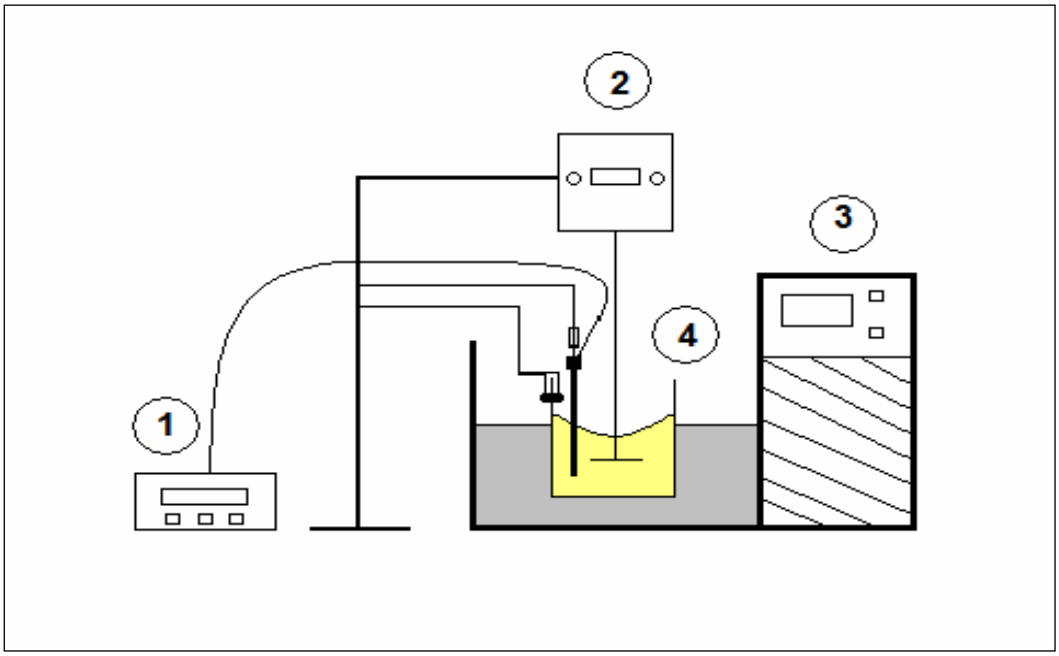

Figure 3.1. The HDP system: 1. pH meter, 2. Stirrer, 3. Heater circulation bath 4. Beaker (Tezcanlı, 2008)

3.2.2. Microreactor Flow System

In microreactor flow system, 1/4″, 1/8″, and 1/16″ OD stainless steel and copper tubing with brass and stainless steel fittings were used. The reactant gases CO, CO_2, He, H_2, O_2 were pressurized from gas cylinders with the optimum pressure of 30 psia. The reactant gases were fed separately to the system with two Brooks 5850E mass flow controllers coupled with 4-Channel Brooks 0154 control panel. All gases used in feed stream were mixed since homogeneous mixing was provided before they entered the reactor tube.

The feed mixture, after being mixed, sent through 4 mm IDx 58.5 cm stainless steel fixed-bed reactor placed in 2.4 cm IDx 50 cm furnace controlled to 0.5± K with an Eurotherm 2408 programmable temperature controller, presented in Figure 3.2. The K-type sheated thermocouple was embedded at the middle of the reactor at a position near the sample to detect the temperature. The distilled water was pumped into the heated gas mixture by using an Agilent 1200 Isocratic HPLC pump. The gases and water mixture entered the reactor tube. The reaction mixture from the exit of the reactor was passed through a cold trap where the water into the feed mixture and produced during the reaction were separated from the product gases.

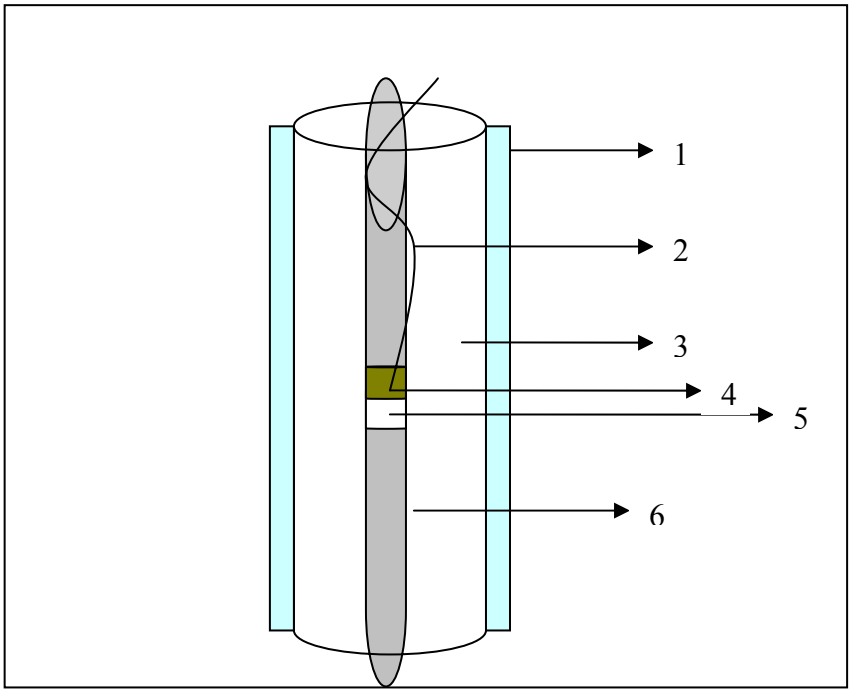

Figure 3.2. Reactor and furnace system: 1.Ceramic wool insulation 2.Thermocouple 3.Furnace 4.Catalyst 5.Catalyst bed 6. Reactor (Tezcanlı, 2008)

3.2.3. Product Analysis System

The feed gas and the product gas stream passed through the cold trap were analyzed using a Hiden Hal 210 mass spectrometer. The microreactor flow and product analysis systems are showed in Figure 3.3.

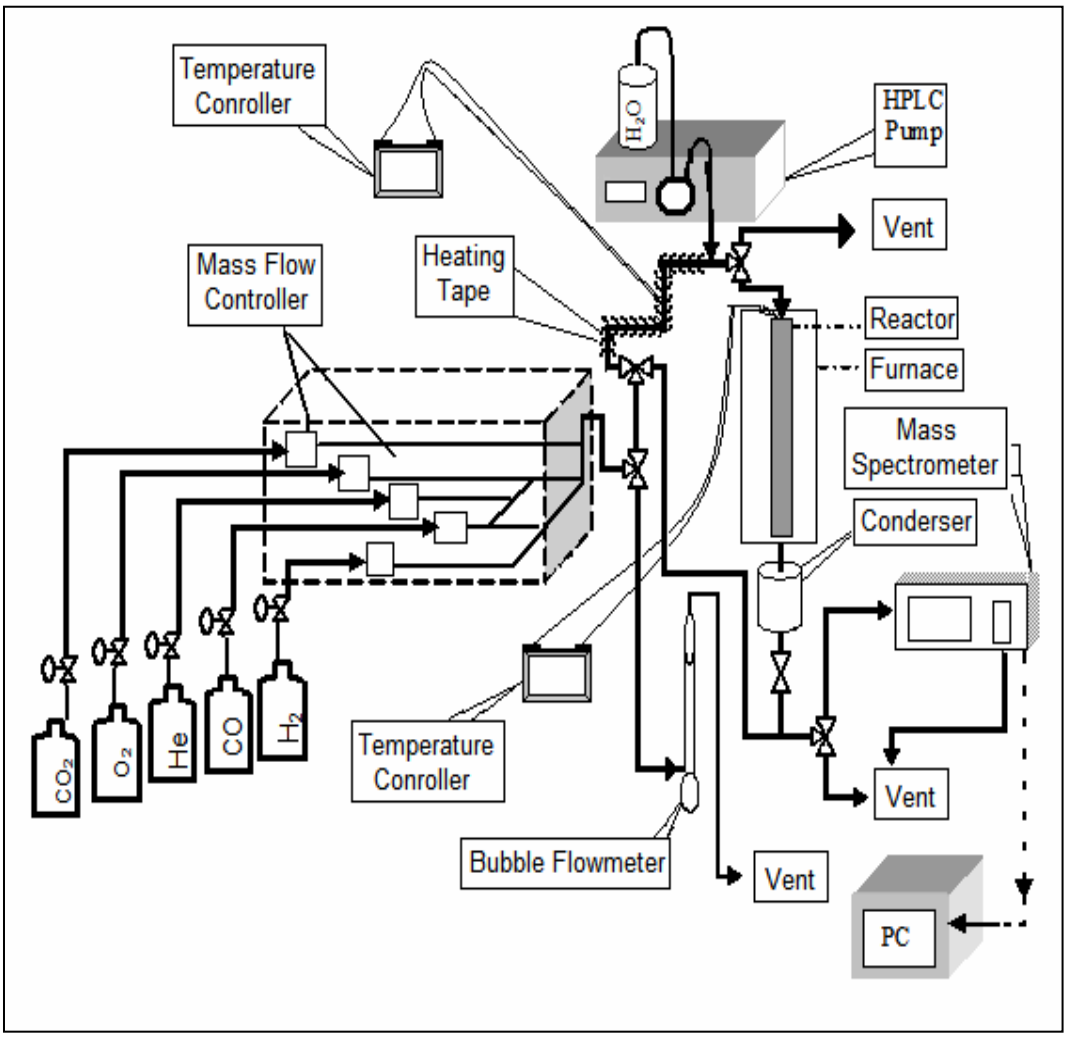

Figure 3.3. The microreactor flow and product analysis system (Tezcanlı, 2008)

3.3. Catalyst Preparation

The catalyst was prepared to obtain the nanosized gold particles over the γ-Al_2O_3 support by using homogeneous deposition precipitation (HDP) method. The experimental set-up for catalyst preparation was presented in Figure 3.1.

Before the synthesis, the alumina support particles were crushed and sieved in order to obtain a powder with 45-60 mesh size (344-255 μm). In order to increase the surface and mechanical properties of the catalysts, a measured amount of support was calcined in a flow of air at 400°C for 2 hours using a heating rate of 5°C/min.

Au loaded over γ-Al_2O_3 catalysts were synthesized by HDP method using urea as precipitating agent. This procedure follows closely by that described by Grisel and Nieuwenhuys (2001b). An aqueous solution of $HAuCl_4.3H_2O$ was used as Au precursor. The precursor was stored in the dark, and the preparations were made in a minimal light in order to avoid possible discoloration of the surface caused by photochemical reactions of the Au precursor. $HAuCl_4.3H_2O$ was dissolved in 25 ml dionized water and then the solution was added to the γ-Al_2O_3 calcinated support suspending in 80 ml dionized water. The pH of aqueous $HAuCl_4.3H_2O$ solution was raised to the desired point by addition of 100 ml solution of an 0.84 M excess urea. The solution was heated to 70°C under vigorously stirring in order to gradually ensure decomposition of the urea. This temperature was kept under these conditions for 4 hours until the pH of the solution reached to 7-8. After aging procedure, the slurry was cooled down, and suction filtered. The catalyst was then washed several times with demineralized water to minimize the amount of remaining Cl^- ions. After the filtration, the catalyst prepared was dried overnight at 100°C.

3.4. Kinetic Measurements

Kinetic tests were carried out in the microreactor flow system presented in Figure 3.2. The experiments were performed over the catalysts reduced in a stream of 50 ml/min H_2 for 30 min at 300°C prior to reaction and kept under a stream of 50 ml/min He until the reaction test was performed. The reduction procedure is given in Table 3.4.

Table 3.4. Reduction program for Au/Al_2O_3 catalyst

Segments	Starting and End Temperatures	Segment Gas
First Segment	Heating from 25˚C to 300˚C with a heating rate of 10ºC/min	H_2 with flow rate of 50 ml/min
Second Segment (Reduction)	Keeping constant at 300˚C for 30 min	H_2 with flow rate of 50 ml/min
Third Segment	Cooling down to reaction temperature	He with flow rate of 25 ml/min

After reduction program, the kinetic tests were performed under a total flow of 100 ml/min using reaction temperature in the 90-130°C range. All kinetic measurements were carried out at atmospheric pressure. In order to limit the conversions to low values, the catalyst samples were diluted with γ-Al_2O_3 into 45-60 mesh size (344-255μm), which is not active for selective CO oxidation under the reaction conditions given in Table 3.5. and Table 3.6. Total bed weight remained constant at 250 mg.

Table 3.5. The reaction conditions for 0.5% Au/Al_2O_3 catalyst in the absence of CO_2 and H_2O at 90-130°C

Total Flow (ml / min)	Weight of Catalyst (mg)	Feed Composition (%) with He as Balance				
		CO	O_2	H_2	H_2O	CO_2
100	5	1	1	60	-	-
100	10	1	1	60	-	-
100	5	1.5	1	60	-	-
100	10	1.5	1	60	-	-
100	5	2	1	60	-	-
100	10	2	1	60	-	-
100	5	2.5	1	60	-	-
100	10	2.5	1	60	-	-
100	5	3	1	60	-	-
100	10	3	1	60	-	-
100	5	1	0.75	60	-	-
100	10	1	0.75	60	-	-
100	5	1	0.6	60	-	-
100	10	1	0.6	60	-	-
100	5	1.5	0.6	60	-	-
100	10	1.5	0.6	60	-	-
100	5	2	0.6	60	-	-
100	10	2	0.6	60	-	-
100	5	2.5	0.6	60	-	-
100	10	2.5	0.6	60	-	-

Table 3.6. The reaction conditions for 1% Au/Al_2O_3 catalyst in the presence of 25% CO_2 and 10% H_2O at 90-130°C

Total Flow (ml / min)	Weight of Catalyst (mg)	Feed Composition (%) with He as Balance				
		CO	O_2	H_2	H_2O	CO_2
100	5	0.75	1	60	10	25
100	10	0.75	1	60	10	25
100	5	1	1	60	10	25
100	10	1	1	60	10	25
100	5	1.5	1	60	10	25
100	10	1.5	1	60	10	25
100	5	2	1	60	10	25
100	10	2	1	60	10	25
100	5	1	0.75	60	10	25
100	10	1	0.75	60	10	25
100	5	1	1.5	60	10	25
100	10	1	1.5	60	10	25
100	5	0.75	0.6	60	10	25
100	10	0.75	0.6	60	10	25
100	5	1	0.6	60	10	25
100	10	1	0.6	60	10	25
100	5	1.5	0.6	60	10	25
100	10	1.5	0.6	60	10	25
100	5	2	0.6	60	10	25
100	10	2	0.6	60	10	25

4. RESULTS AND DISCUSSION

The scope of this study was to determine kinetic model for selective CO oxidation over Au/Al_2O_3 catalyst. The kinetic experiments were studied in the absence and the presence of 10 per cent H_2O and 25 per cent CO_2 in the feed stream. The CO conversion (x_{CO}) is defined based on the CO_2 formation as follows;

$$\text{CO conversion}\,(\%) = \frac{[\text{CO}]_{\text{in}} - [\text{CO}]_{\text{out}}}{[\text{CO}]_{\text{in}}} \times 100 \tag{4.1}$$

The amount of liquid water used in the experiments is calculated as below;

$$V_{Steam(H_2O)} = \frac{V_{Liquid(H_2O)} \times \rho_{H_2O} \times R \times T}{MW_{H_2O} \times P} \tag{4.2}$$

where ρ=1000 $g.L^{-1}$; P=1 atm; R=0.082 $L.atm.mol^{-1}.K^{-1}$; T=298 K and MW_{H2O}=18 $g.mol^{-1}$.

4.1. Possible Reaction Mechanisms of CO Oxidation

To date, several studies have been reported for the kinetics and mechanism for CO oxidation over supported Au catalysts. The rate expressions were constructed using the mechanisms reported in the literature.

In spite of rare studies of CO_2 effects on CO oxidation over Au catalyst, it is found that addition of H_2O and CO_2 together has a negative effect on the CO oxidation rate (Schubert *et. al*., 2004; Tezcanlı, 2008). In this work, the effects of the presence of H_2O and CO_2 in the feed stream on the reaction rate parameters were considered. However the reaction involved these two feed components, as reactants, was neglected to avoid complications.

Although many debates occur on the adsorption of O_2, it is generally accepted that molecular O_2 is adsorbed on Au surfaces at low temperatures because dissociative adsorption of O_2 into adsorbed atomic oxygen may be energetically unfavorable. However, in the presence of a support, the adsorption of atomic oxygen can proceed at the metal-support interface; hence, the adsorption of oxygen may become favorable (Kung *et. al.*, 2004).

Al_2O_3 is an inert support, it is therefore considered that reaction mechanisms for CO oxidation on Au/Al_2O_3 catalyst consist of only monofunctional paths carried out on the gold sites.

Haruta and Date (2001) proposed that the reaction mechanisms for CO oxidation over gold catalysts varied with the temperatures. The reaction occured at below -73°C, was consistent with the Langmuir-Hinselwood kinetics, involving both CO adsorption and O_2 adsorption on the surface of Au and then a reaction of adsorbed CO with adsorbed O_2 molecule followed by the reaction of another adsorbed CO on the Au surface with the remaining adsorbed oxygen atom. These reactions are presented as steps (1) to (4) in Table 4.1., where "a" denotes an adsorption site on Au surface. The rate expression for the mechanism proposed by Haruta and Date for these four steps is given in Equation (4.3). As the reaction between CO adsorbed on the Au surface and atomic oxygen adsorbed on the Au surface is fast, i.e. $k_4 >> k_3$, the rate expression becomes a simplified form in Equation (4.4).

$$-r_{CO} = \frac{(2k_2P_{O_2})(K_1k_3k_4P_{CO}[S]_0 - k_2k_4P_{O_2} - k_2k_3P_{O_2})}{K_1k_3k_4P_{CO}(K_1P_{CO}+1)} \tag{4.3}$$

$$-r_{CO} = \frac{(k_2P_{O_2})(K_1k_3P_{CO}[S]_0 - k_2P_{O_2})}{K_1k_3P_{CO}(K_1P_{CO}+1)} \tag{4.4}$$

Table 4.1. Elementary steps of possible reaction mechanism for CO oxidation over $AuAl_2O_3$ (Haruta and Date, 2001)

Elementary Step	Step Number
$CO + a \underset{k_{-1}}{\overset{k_1}{\Leftrightarrow}} COa$	(1)
$O_2 + a \xrightarrow{k_2} O_2a$	(2)
$COa + O_2a \xrightarrow{k_3} CO_2 + Oa + a$	(3)
$COa + Oa \xrightarrow{k_4} CO_2 + 2a$	(4)
$COa + O_2a \xrightarrow{k_5} CO_3a + a$	(5)
$CO_3a \xrightarrow{k_6} CO_2 + Oa$	(6)

In one-site reaction model suggested by Haruta and Date (2001) for the temperatures between -73°C and 27°C, on the other hand, the reaction proceeds through the formation of a carbonate intermediate. Davran-Candan *et. al.* (2009) also proposed the mechanism leading to the formation of CO-OO intermediate. The CO reversibly and O_2 irreversibly are adsorbed on the Au surface similar to the previous mechanism, i.e. steps (1) and (2) in Table 4.1. The reaction takes place at the Au surface to form carbonate species ($-CO_3$) in step (5) and formation of first CO_2 in step (6) in Table 4.1. Assuming that the atomic oxygen adsorbed on the Au site reacts with CO adsorbed as in step (4), the rate expression for the reaction model for CO oxidation takes the following form;

$$-r_{CO} = \frac{2K_1k_2k_5k_6P_{CO}P_{O_2}[S]_0}{K_1k_5k_6P_{CO}(K_1P_{CO}+1) + k_2k_6P_{O_2} + K_1k_2k_5P_{CO}P_{O_2}} \tag{4.5}$$

In one-site model suggested by Tseng *et. al*. (2009), CO oxidation reaction is elucidated using the Langmuir-Hinselwood mechanism (Table 4.2.). The adsorption of O_2 is rate limiting and consists of two steps; direct adsorption of O_2 molecule on Au particles and the breaking of O-O bonds on Au sites, i.e. steps (2) and (3) in Table 4.2. As the atomic oxygen reacts with CO adsorbed on the Au surface, i.e. step (4), the rate expression for the reaction becomes the one shown in Equation (4.6). Assuming that molecular O_2

chemisorption is slower than dissociation of O_2 and neglecting the terms having smaller values in the Equation (4.6), the rate expression is simplified to Equation (4.7) which has essentially the same form with Equation (4.4).

$$-r_{CO} = \frac{(2k_2P_{O_2})(K_1k_3k_6P_{CO}[S]_0 - K_1k_2k_6P_{CO}P_{O_2} - 2k_2k_3P_{O_2})}{K_1k_3k_6P_{CO}(K_1P_{CO}+1)} \tag{4.6}$$

$$-r_{CO} = \frac{(2k_2P_{O_2})(K_1k_3k_6P_{CO}[S]_0 - 2k_2k_3P_{O_2})}{K_1k_3k_6P_{CO}(K_1P_{CO}+1)} \tag{4.7}$$

Assuming that adsorption of O_2 molecule on the surface of Au is considered to be rate limiting step, i.e. $k_3 >> k_2$ in Table 4.2., and the surface of Au is completely covered with CO, i.e. [COS]>>[S], the rate expression for one-site model proposed by Tseng *et. al*. (2009) becomes the form in Equation (4.8).

$$-r_{CO} = \frac{2k_2P_{O_2}[S]_0}{K_1P_{CO}+1} \tag{4.8}$$

Table 4.2. Elementary steps of the mechanism for CO oxidation over Au/Fe_3O_4 (Tseng *et al*., 2009)

Elementary Step	Step Number
$CO + a \underset{k_{-1}}{\overset{k_1}{\Leftrightarrow}} COa$	(1)
$O_2 + a \overset{k_2}{\rightarrow} O_2a$	(2)
$O_2a + a \overset{k_3}{\rightarrow} 2Oa$	(3)
$COa + Oa \overset{k_6}{\rightarrow} CO_2 + 2a$	(4)

Gottfried and Christmann (2004) suggested that CO oxidation proceeds through a pathway consistent with the Langmuir-Hinselwood mechanism, in the high temperature range. In their one-site mechanism, CO and O_2 are reversibly adsorbed on Au particles, followed by reversible separation of O_2 on Au surface, presented in Table 2.1. Assuming

that the CO_2 equilibrium coverage is very low and the equilibrium CO coverage is low with an excess of gas phase CO, θ_{CO} and θ_{CO_2} can be neglected in the rate expression. Then the following rate expression is given;

$$r_{CO_2} = K_{a,CO} k_r P_{CO} \theta_O * \tag{4.9}$$

In order to give similarities between Michaelis-Menten (M-M) enzyme kinetics and kinetics of heterogeneous catalysts, Long *et. al*. (2008) applied some of the M-M principles to CO oxidation over supported Au catalysts. In this study, it is believed that CO binding on Au surface is fast and O_2 is irreversibly adsorbed on the Au surface, as rate determining step i.e. step (2) in Table 4.3., followed by the reaction occuring with available CO to yield CO_2, i.e. step (3). As the following step, i.e. step (4), to produce CO_2 in Table 4.3., is considered to be kinetically unobservable, the rate expression is simplified to Equation (4.10), where ν_{max} is analogous to the maximum velocity in M-M kinetics.

$$-r_{CO} = \frac{\nu_{\max} P_{O_2}}{K_2 + P_{O_2}} \tag{4.10}$$

Table 4.3 Elementary steps of the mechanism for CO oxidation over supported Au catalysts (Long *et al*., 2008)

Elementary Step	Step Number
$2CO + 2a \underset{k_{-1}}{\overset{k_1}{\Leftrightarrow}} 2COa$	(1)
$O_2 + a \overset{k_2}{\rightarrow} O_2a$	(2)
$COa + O_2a \overset{k_3}{\rightarrow} CO_2 + Oa + a$	(3)
$COa + Oa \overset{k_4}{\rightarrow} CO_2 + 2a$	(4)

4.2. Experimental Results

CO conversion values for CO oxidation rates were obtained using ten reaction mixtures at three different temperatures both in the absence and presence of CO_2 and H_2O, and the rate expressions were proposed from mechanisms in the literature for CO oxidation reaction over supported Au catalysts. In order to estimate the kinetic constants, small amounts of catalyst, i.e. 5mg and 10 mg, were mixed with inert Al_2O_3 supports, so were to help CO conversion be kept at low values.

4.2.1. The Effects of CO and O_2 Concentrations on CO Conversion

Selective CO oxidation over Au/Al_2O_3 catalysts were carried out in the absence and the presence of 10% H_2O and 25% CO_2 at temperature ranging 90°C to 130°C in order to examine the effects of CO and O_2 concentrations on the CO conversion.

4.2.1.1. The Effects of CO and O_2 Concentrations in the Absence of H_2O and CO_2; The first study of CO oxidation over Au/Al_2O_3 catalyst was performed in the absence of H_2O and CO_2.

As seen in Table 4.4., CO conversion decreases with decreasing content of Au and there were no significant changes between the activity of 0.3 per cent Au/Al_2O_3 catalyst and 0.5 per cent Au/Al_2O_3 catalyst using 10 mg catalyst. Hence 0.5 per cent Au is selected because the conversion level obtained with 1% is too high for kinetic studies and 0.3 per cent catalyst may have cause some operational problems such as weighting, mixing with the support and so on.

Table 4.4. Effects of Au content on CO conversion in the absence of H_2O and CO_2 at 1% CO, 1% O_2, 60% H_2 and balance He

Au Content (%)	CO Conversion (x_{CO})		
	T=90°C	T=110°C	T=130°C
0.3	0.26	0.35	0.34
0.5	0.25	0.34	0.33
1	0.35	0.43	0.30

Table 4.5. indicates that the increase in CO concentration results in decreasing CO conversion because reduces the active sites for the adsorption of O_2. As the O_2 concentration increases continuously, CO conversion also increases. However, the higher O_2 concentrations also increase the oxidation of H_2 and decrease in CO_2 selectivity; therefore, it is very important to attain optimum O_2/CO ratios.

Table 4.5. Experimental results of kinetics on CO oxidation kinetics for different CO and O_2 concentrations in the absence of CO_2 and H_2O measured at 60% H_2, and balance He at temperature ranging 90°C to 130°C

			[a]W_{CAT} / [b]F_{CO} (mg.s.μmol^{-1})			[c]X_{CO} (fractional)		
Exp. No.	CO (mol %)	O_2 (mol %)	90°C	110°C	130°C	90°C	110°C	130°C
1	1.5	1	5.962	6.289	6.617	0.11	0.17	0.16
2			11.924	12.579	13.235	0.19	0.27	0.25
3	2	1	4.471	4.717	4.963	0.08	0.12	0.13
4			8.943	9.434	9.926	0.14	0.20	0.18
5	2.5	1	3.576	3.774	3.970	0.05	0.07	0.08
6			7.152	7.548	7.940	0.12	0.17	0.15
7	3	1	2.981	3.145	3.308	0.03	0.05	0.04
8			5.962	6.290	6.616	0.10	0.14	0.13
9	1	0.6	8.943	9.434	9.926	0.09	0.14	0.16
10			17.886	18.868	19.853	0.17	0.26	0.22
11	1	0.75	8.943	9.434	9.926	0.11	0.17	0.19
12			17.886	18.868	19.853	0.18	0.27	0.25
13	1	1	8.943	9.434	9.926	0.17	0.19	0.18
14			17.886	18.868	19.853	0.25	0.34	0.33
15	1.5	0.6	5.962	6.289	6.617	0.05	0.07	0.06
16			11.924	12.579	13.235	0.12	0.17	0.16
17	2	0.6	4.471	4.717	4.963	0.03	0.06	0.05
18			8.943	9.434	9.926	0.09	0.12	0.12
19	2.5	0.6	3.576	3.774	3.970	0.02	0.04	0.05
20			7.152	7.548	7.940	0.07	0.10	0.09

[a]Catalyst weight, [b]CO flow rate, [c]CO conversion

4.2.1.2. The Effects of CO and O_2 Concentrations in the Presence of H_2O and CO_2; In order to study the effects of CO and O_2 concentrations in the presence of H_2O and CO_2, 1

wt.% Au/Al_2O_3 catalyst was used. The kinetic experiments were carried out using various O_2/CO ratios between 1.5 and 0.5.

Table 4.6. shows that CO conversion decreases with increasing CO concentration, varied from 0.75 per cent to 2 per cent, while O_2 concentration is kept constant (1% and 0.6%) in the feed stream. Additionally, CO conversion increases with increasing the weight of catalyst; the CO conversion reaches maximum values as CO concentration is 0.75 per cent in the feed stream. However, at higher concentrations of CO, there is a decrease in CO conversion because CO can block the active sites and prevent the adsorption of O_2. At high O_2 concentrations, CO conversion increases with increasing O_2 concentration because the higher O_2/CO ratio provides complete oxidation of CO. However, the excess O_2 also increases H_2 oxidation (Mozer *et. al*., 2009).

The effects of CO and O_2 concentrations are similar to those in the absence of H_2O and CO_2 in the feed stream, but the addition of H_2O and CO_2 lowered CO conversion apperantly due to the strong adsorption of these components on the active sites. (Luengnaruemitchai *et. al.*, 2004). Yu *et. al.* (2007) reported that lower CO conversion values were obtained in the presence of 3 per cent H_2O and 15 per cent CO in the feed than that in the absence of H_2O and CO_2 at higher temperatures than 50°C. Although the addition of small concentrations of H_2O (200 ppm) has a positive effect on CO conversion, its increasing concentration reduces the activity of the catalyst (Date and Haruta, 2001).

Table 4.6. Experimental results of kinetics on CO oxidation in the presence of 10% H_2O and 25% CO_2 measured at 60% H_2, and balance He

			[a]W_{CAT} / [b]F_{CO} (mg.s.μmol^{-1})			[c]X_{CO} (fractional)		
Exp. No.	CO (mol %)	O_2 (mol %)	90°C	110°C	130°C	90°C	110°C	130°C
1	0.75	1	11.924	12.579	13.235	0.05	0.08	0.13
2			23.848	25.157	26.470	0.12	0.26	0.25
3	1	1	8.943	9.434	9.926	0.03	0.07	0.09
4			17.886	18.868	19.853	0.07	0.17	0.19
5	1.5	1	5.962	6.289	6.617	0.02	0.04	0.07
6			11.924	12.579	13.235	0.04	0.11	0.12
7	2	1	4.471	4.717	4.963	0.01	0.05	0.06
8			8.943	9.434	9.926	0.02	0.07	0.08
9	1	0.75	8.943	9.434	9.926	0.02	0.04	0.08
10			17.886	18.868	19.853	0.05	0.12	0.18
11	1	1.5	8.943	9.434	9.926	0.06	0.07	0.14
12			17.886	18.868	19.853	0.1	0.18	0.25
13	0.75	0.6	11.924	12.579	13.235	0.04	0.07	0.08
14			23.848	25.157	26.470	0.07	0.11	0.12
15	1	0.6	8.943	9.434	9.926	0.03	0.04	0.06
16			17.886	18.868	19.853	0.05	0.09	0.08
17	1.5	0.6	5.962	6.289	6.617	0.01	0.02	0.03
18			11.924	12.579	13.235	0.02	0.05	0.06
19	2	0.6	4.471	4.717	4.963	0.01	0.02	0.02
20			8.943	9.434	9.926	0.02	0.03	0.04

[a]Catalyst weight, [b]CO flow rate, [c]CO conversion

4.3. Rate Calculations

The reaction rates were obtained from the data in Table 4.5. and 4.6. by using differential method, where conversion was kept at lower values using the small amounts of catalyst (5-10 mg).

The reaction rates of CO consumption were individually calculated from the slope of the conversion versus space time (W/F_{CO}) plots. Each plot showed a straight line fitting for each reaction rate. In each set of kinetic experiments, ten different CO and O_2 concentrations were used for three different temperatures at constant feed flow.

4.3.1. Rate Calculations in the Absence of H_2O and CO_2

The initial rates determined from the data in kinetic experiments in the absence of H_2O and CO_2 were shown in Figure 4.1. for 90°C, Figure 4.2. for 110°C and Figure 4.3. for 130°C and tabulated in Table 4.7. as a summary.

Table 4.7. indicates that O_2 concentration has a positive effect on reaction rate. However, the opposite effect was observed at high CO concentration, where reaction rate decreases with increasing CO concentration.

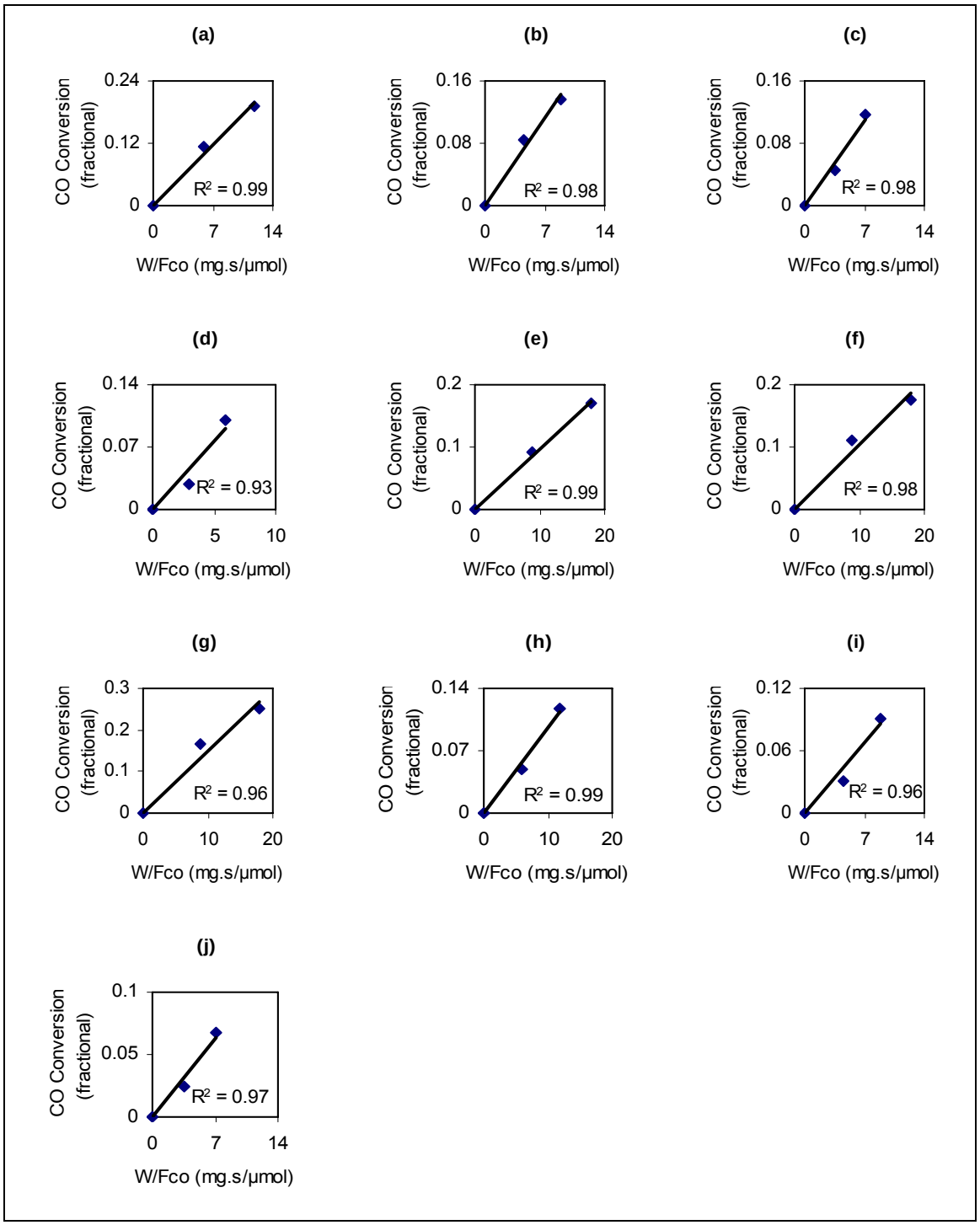

Figure 4.1. Fractional CO conversion vs. space time (W/F_{CO}) graphs: (a) 1.5% CO, 1% O_2; (b) 2% CO, 1% O_2; (c) 2.5% CO, 1% O_2; (d) 3% CO, 1% O_2; (e) 1% CO, 0.6% O_2; (f) 1% CO, 0.75% O_2; (g) 1% CO, 1% O_2; (h) 1.5% CO, 0.6% O_2; (i) 2% CO, 0.6%O_2; (j) 2.5% CO, 0.6% O_2 in the absence of CO_2 and H_2O in the feed at 90°C

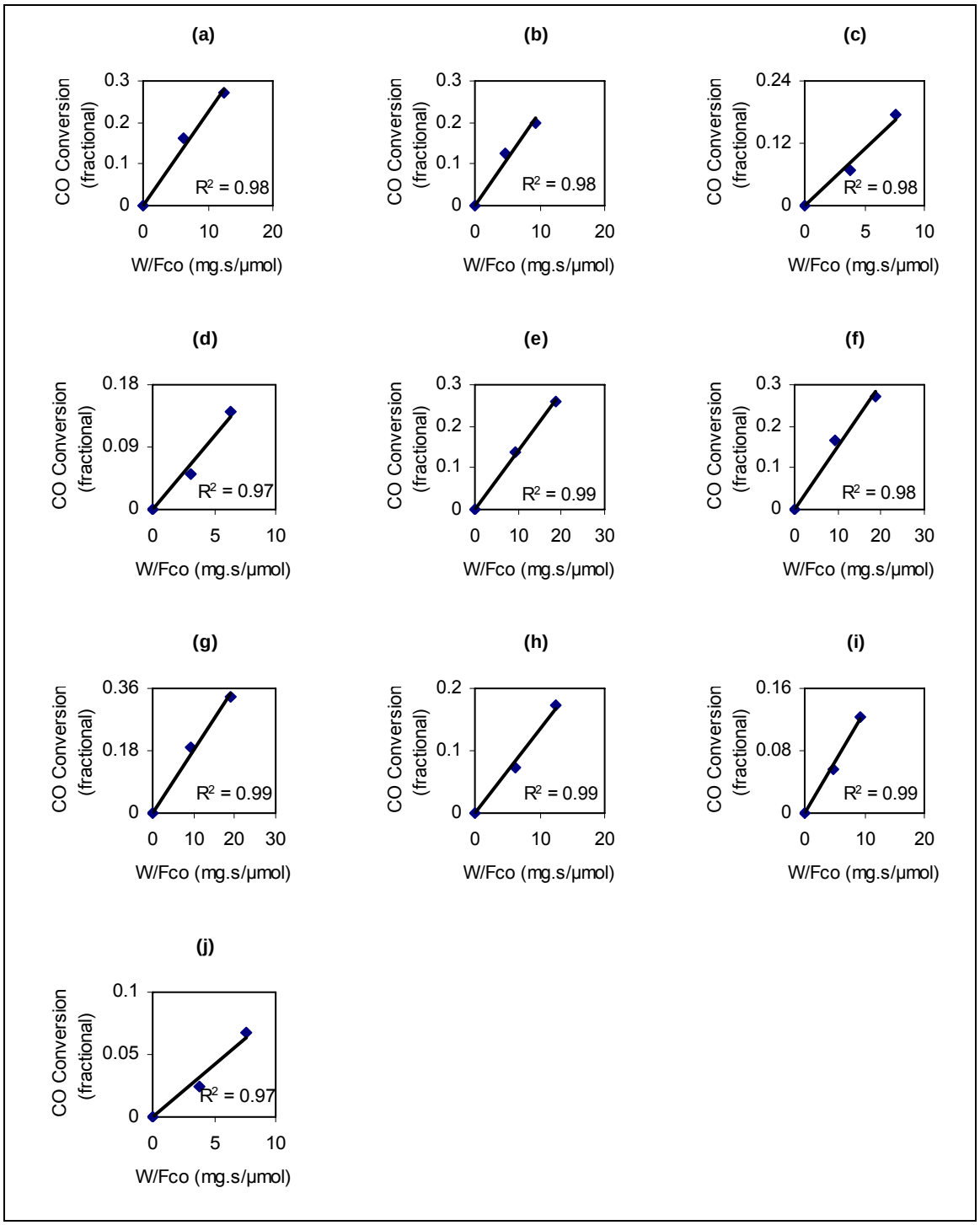

Figure 4.2. Fractional CO conversion vs. space time (W/F_{CO}) graphs: (a) 1.5% CO, 1% O_2; (b) 2% CO, 1% O_2; (c) 2.5% CO, 1% O_2; (d) 3% CO, 1% O_2; (e) 1% CO, 0.6% O_2; (f) 1% CO, 0.75% O_2; (g) 1% CO, 1% O_2; (h) 1.5% CO, 0.6% O_2; (i) 2% CO, 0.6%O_2; (j) 2.5% CO, 0.6% O_2 in the absence of CO_2 and H_2O in the feed at 110°C

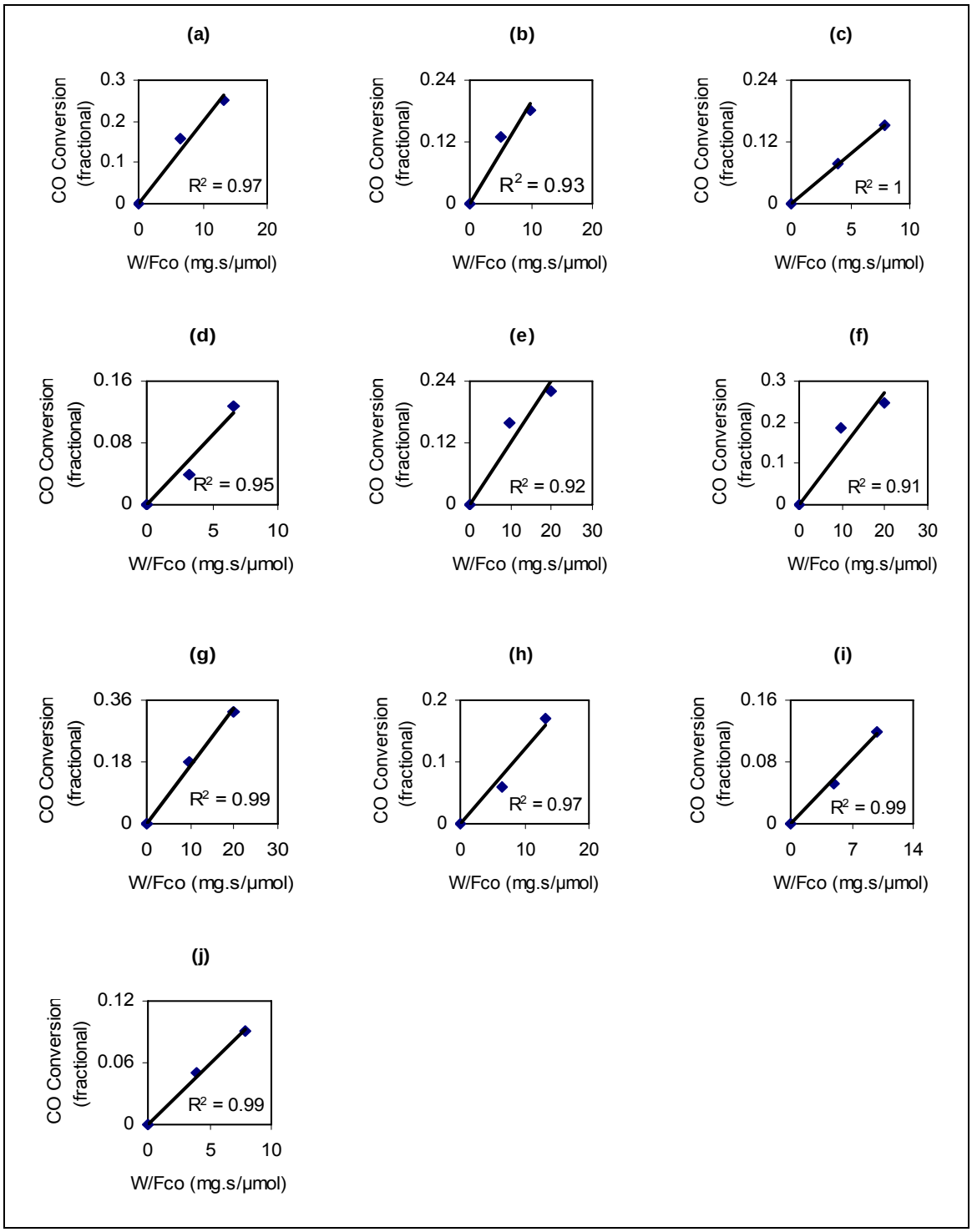

Figure 4.3. Fractional CO conversion vs. space time (W/F_{CO}) graphs: (a) 1.5% CO, 1% O_2; (b) 2% CO, 1% O_2; (c) 2.5% CO, 1% O_2; (d) 3% CO, 1% O_2; (e) 1% CO, 0.6% O_2; (f) 1% CO, 0.75% O_2; (g) 1% CO, 1% O_2; (h) 1.5% CO, 0.6% O_2; (i) 2% CO, 0.6%O_2; (j) 2.5% CO, 0.6% O_2 in the absence of CO_2 and H_2O in the feed at 130°C

Table 4.7. Initial rates calculated from CO conversion vs. W/F_{CO} data in the absence of CO_2 and H_2O, measured at 60% H_2, and balance He

Experiment No.	CO (mol %)	O_2 (mol %)	Reaction rate ($\mu mol\ mg^{-1}s^{-1}$) T=90°C	Reaction rate ($\mu mol\ mg^{-1}s^{-1}$) T=110°C	Reaction rate ($\mu mol\ mg^{-1}s^{-1}$) T=130°C
1-2	1.5	1	0.0165	0.0224	0.0199
3-4	2	1	0.0161	0.0222	0.0197
5-6	2.5	1	0.0155	0.0221	0.0192
7-8	3	1	0.0153	0.0212	0.0179
9-10	1	0.6	0.0097	0.0140	0.0121
11-12	1	0.75	0.0104	0.0151	0.0137
13-14	1	1	0.0150	0.0183	0.0168
15-16	1.5	0.6	0.0096	0.0134	0.0121
17-18	2	0.6	0.0095	0.0128	0.0117
19-20	2.5	0.6	0.0089	0.0128	0.0116

4.3.2. Rate Calculations in the Presence of H_2O and CO_2

The initial rates determined from the data in the kinetic experiments in the presence of H_2O and CO_2 were presented in Figure 4.4. for 90°C, Figure 4.5. for 110°C and Figure 4.6. for 130°C, and summarized in Table 4.8. and by differentiation and extrapolation to zero space time.

As illustrated in Table 4.8., O_2 concentration has a positive effect on the reaction rate, while CO concentration negatively affects the reaction rate. Compared to rates in the absence of H_2O and CO_2 in the feed stream, reaction rates had lower values in the presence of 10 per cent H_2O and 25 per cent CO_2.

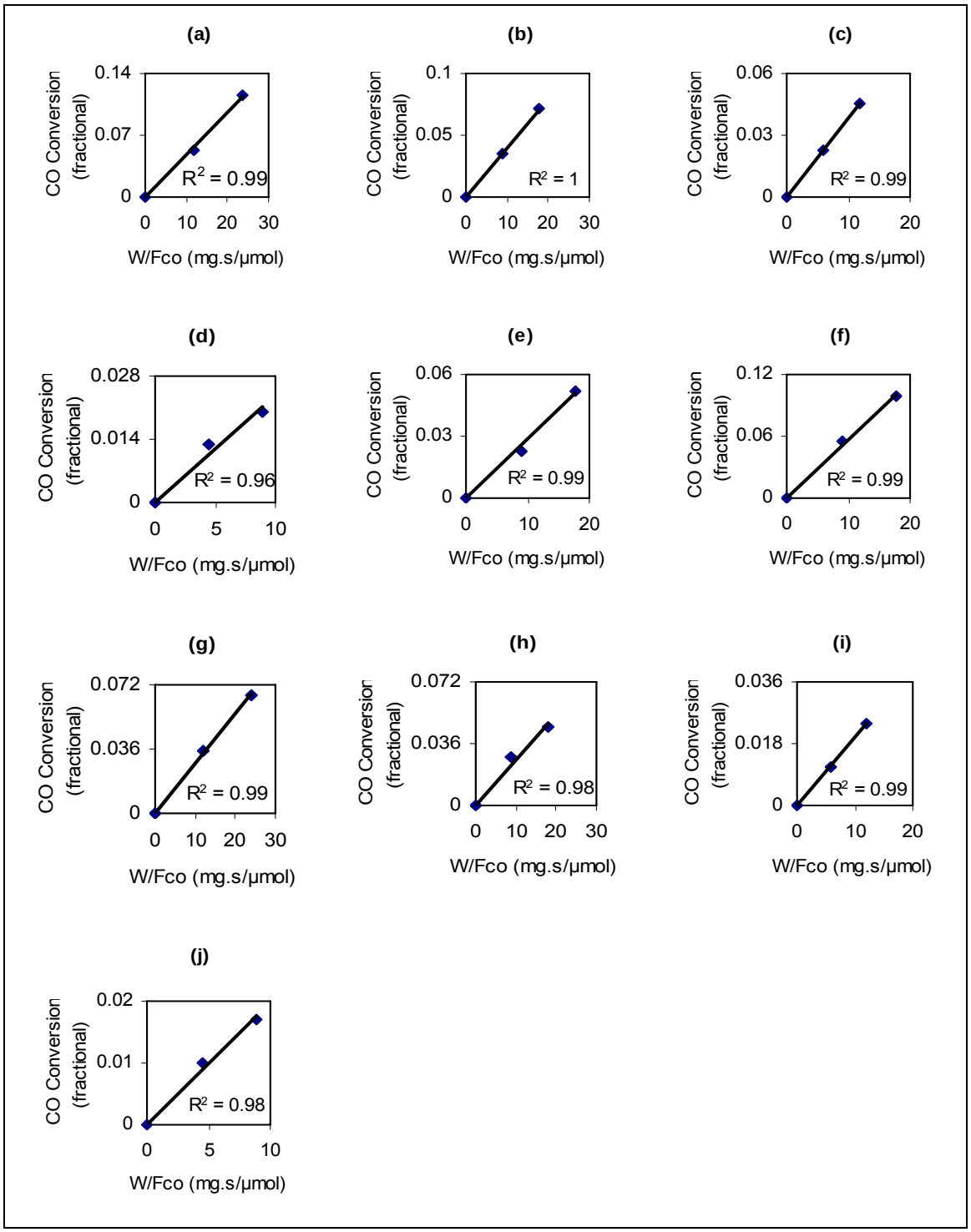

Figure 4.4. Fractional CO conversion vs. space time (W/F_{CO}) graphs: (a) 0.75% CO, 1% O_2; (b) 1% CO, 1% O_2; (c) 1.5% CO, 1% O_2; (d) 2% CO, 1% O_2; (e) 1% CO, 0.75% O_2; (f) 1% CO, 1.5% O_2; (g) 0.75% CO, 0.6% O_2; (h) 1% CO, 0.6% O_2; (i) 1.5% CO, 0.6% O_2; (j) 2% CO, 0.6% O_2 in the presence of 25% CO_2 and 10% H_2O in the feed at 90°C

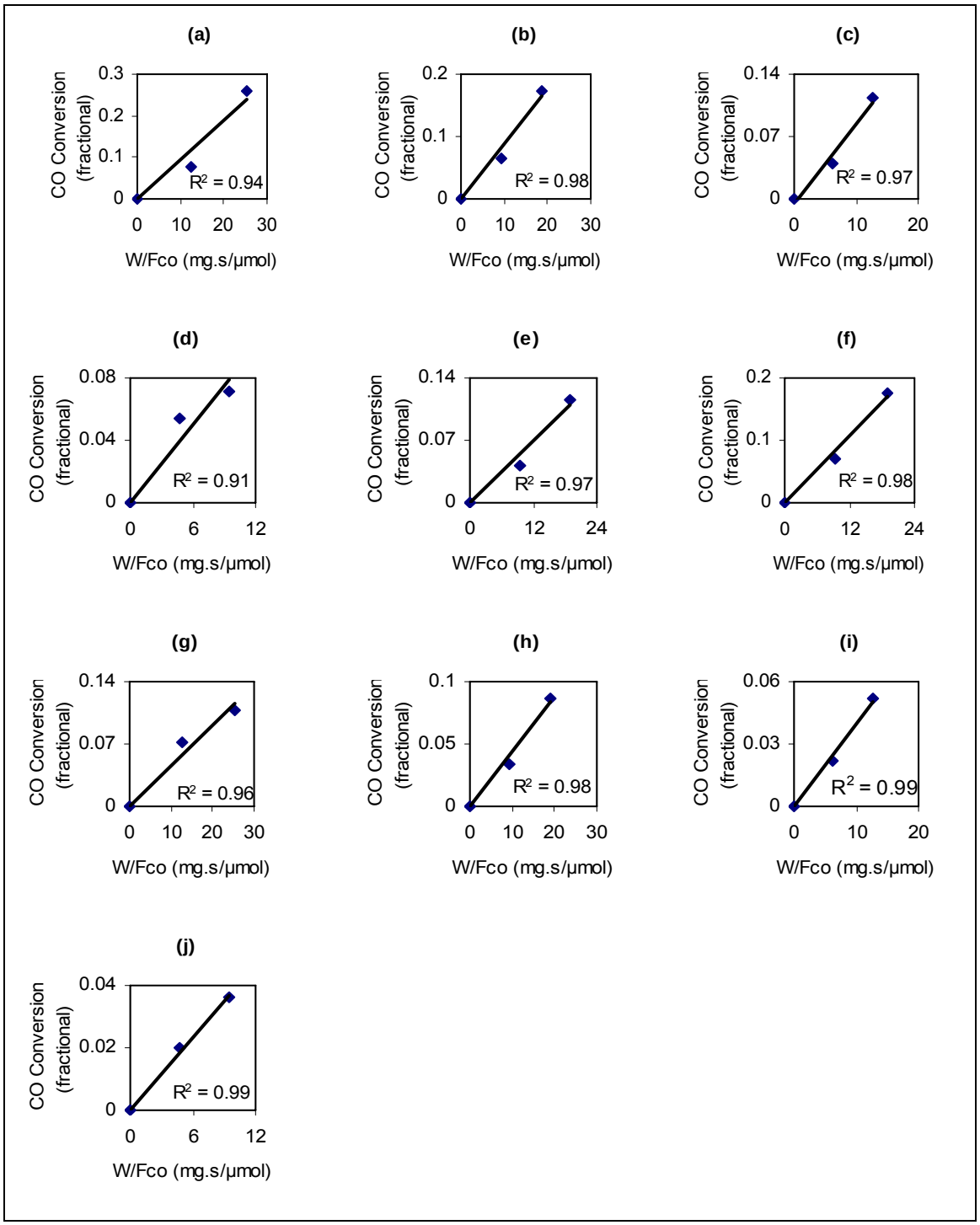

Figure 4.5. Fractional CO conversion vs. space time (W/F_{CO}) graphs: (a) 0.75% CO, 1% O_2; (b) 1% CO, 1% O_2; (c) 1.5% CO, 1% O_2; (d) 2% CO, 1% O_2; (e) 1% CO, 0.75% O_2; (f) 1% CO, 1.5% O_2; (g) 0.75% CO, 0.6% O_2; (h) 1% CO, 0.6% O_2; (i) 1.5% CO, 0.6% O_2; (j) 2% CO, 0.6% O_2 in the presence of 25% CO_2 and 10% H_2O in the feed at 110°C

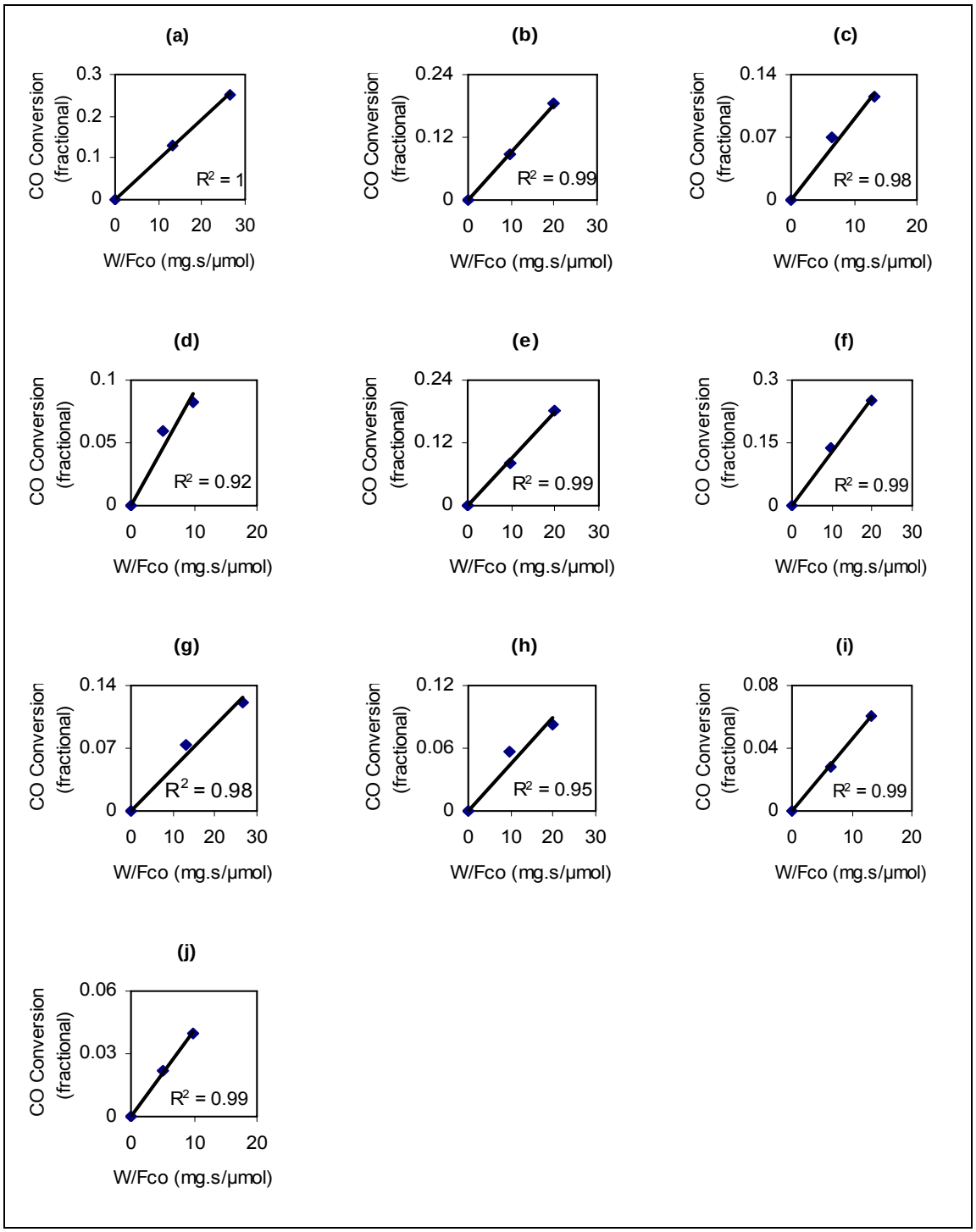

Figure 4.6. Fractional CO conversion vs. space time (W/F_{CO}) graphs: (a) 0.75% CO, 1% O_2; (b) 1% CO, 1% O_2; (c) 1.5% CO, 1% O_2; (d) 2% CO, 1% O_2; (e) 1% CO, 0.75% O_2; (f) 1% CO, 1.5% O_2; (g) 0.75% CO, 0.6% O_2; (h) 1% CO, 0.6% O_2; (i) 1.5% CO, 0.6%O_2; (j) 2% CO, 0.6% O_2 in the presence of 25% CO_2 and 10% H_2O in the feed at 130°C

Table 4.8. Initial rates calculated from CO conversion vs. W/F_{CO} data in the presence of 25% CO_2 and 10% H_2O, measured at 60% H_2, and balance He

Experiment No.	CO (mol %)	O_2 (mol %)	Reaction rate (μmol $mg^{-1}s^{-1}$) T=90°C	Reaction rate (μmol $mg^{-1}s^{-1}$) T=110°C	Reaction rate (μmol $mg^{-1}s^{-1}$) T=130°C
1-2	0.75	1	0.0048	0.0097	0.0096
3-4	1	1	0.0040	0.0087	0.0092
5-6	1.5	1	0.0038	0.0085	0.0091
7-8	2	1	0.0024	0.0083	0.0090
9-10	1	0.75	0.0028	0.0058	0.0089
11-12	1	1.5	0.0057	0.0090	0.0128
13-14	0.75	0.6	0.0028	0.0055	0.0048
15-16	1	0.6	0.0027	0.0053	0.0045
17-18	1.5	0.6	0.0020	0.0051	0.0045
19-20	2	0.6	0.0020	0.0039	0.0041

4.4. Parameter Estimation and Model Discrimination

The kinetic parameters for CO oxidation given in the rate expressions explained in Section 4.1. were obtained by the initial concentrations of CO and O_2 converted into partial pressure at atmospheric pressure (1 atm). The parameters for each experiment set were estimated at temperatures ranging from 90 to 130°C using non-linear least squares methods leading to the positive parameters and minimizing the following function;

$$S(b) = \left(\sum_{i=1}^{n} [y_i - f(x_i, \beta)]^2 \right) Minimize \tag{4.11}$$

where S is the objective function, β is the parameter vector, y_i is the experimentally measured value, $f(x_i, \beta)$ is the model calculated value, x_i is the vector of set of variables for experiment i, and n is the number of individual experiments. Independent and dependent variables (y_i, x_i) optimize the parameter β of the model, so that the sum of the squares of the deviations becomes minimal. For this purpose, the Levenberg-Marquardt regression was coded using LSQNONLIN subroutine function in MATLAB 7.4.0 (2007). In order to use the iterative procedures, starting values for unknown parameters are provided before the software begins the optimization. The starting values must be reasonably close to the unknown parameter estimates.The kinetic parameters given in the rate expressions were represented as the forms used in MATLAB code, listed in Table 4.9.

Table 4.9. The kinetic parameters represented as the forms used in MATLAB code

	Kinetic Parameters				
Model Eqns.	K1	K2	K3	K4	K5
4.3	$K_1k_2k_3k_4[S]_0$	k_2k_4	k_2k_3	$K_1{}^2k_3k_4$	$K_1\ k_3k_4$
4.4	$K_1k_2k_3[S]_0$	k_2	$K_1{}^2k_3$	$K_1\ k_3$	-
4.5	$K_1k_2k_5k_6[S]_0$	$K_1k_5k_6$	$K_1{}^2k_5k_6$	k_2k_3	$K_1k_2k_5$
4.6	$K_1k_2k_3k_6[S]_0$	$K_1k_2k_6$	k_2k_3	$K_1{}^2k_3k_6$	$K_1k_3k_6$
4.7	$K_1k_2k_3k_6[S]_0$	k_2k_3	$K_1{}^2k_3k_6$	$K_1k_3k_6$	-
4.8	k_2	K_1	-	-	-
4.9	$K_{a,CO}k_r\theta_o$ *	-	-	-	-
4.10	$\nu_{\max}$	K_2	-	-	-
4.12	k	-	-	-	-
4.13	k	-	-	-	-

4.4.1. Parameter Estimation in the Absence of H_2O and CO_2

Taking the results obtained after the regression analysis into account, all the model equations had positive parameters making the discrimination diffucult. However, the rates calculated by only six model equations, i.e. Equation (4.3), (4.4), (4.5), (4.7), (4.8) and (4.11), indicate to be in good agreement with experimentally measured rates as given in Table 4.10., Equation (4.6) exhibits a good fit between calculated and experimental rates, Equation (4.7) and (4.8) simplified forms of Equation (4.6) have higher R^2 values and contain no term about dissociation. It is therefore considered that the reaction involving dissociation of O_2 is not carried out. The parameters calculated using the MATLAB code for the plausible rate equations are given in Table 4.11., Table 4.12. and Table 4.13. in the absence of H_2O and CO_2 for temperatures 90°C, 110°C and 130°C, respectively.

Table 4.10. Regression coefficients for model equations

	R^2 values in the absence of H_2O and CO_2			R^2 values In the presence of H_2O and CO_2		
Model Eqns.	90°C	110°C	130°C	90°C	110°C	130°C
4.3	0.974	0.974	0.989	0.936	0.841	0.918
4.4	0.977	0.984	0.990	0.952	0.880	0.924
4.5	0.976	0.967	0.982	0.944	0.845	0.906
4.6	0.921	0.911	0.951	0.900	0.804	0.900
4.7	0.974	0.975	0.986	0.946	0.853	0.921
4.8	0.955	0.917	0.931	0.946	0.904	0.901
4.9	0.049	0.091	0.061	0.245	0.237	0.054
4.10	0.940	0.910	0.920	0.739	0.599	0.748
4.12	0.966	0.971	0.950	-	-	-
4.13	-	-	-	0.953	0.961	0.942

Table 4.11. The kinetic parameters calculated in the model equations in the absence of H_2O and CO_2 at 90°C

	Kinetic Parameters				
Model Eqn.	K1	K2	K3	K4	K5
4.3	1.576 $\left[\frac{\mu mol}{mg.s.kPa^2}\right]$	0.129 $\left[\frac{\mu mol}{mg.s.kPa^2}\right]$	0.142 $\left[\frac{\mu mol}{mg.s.kPa^2}\right]$	8.775 $\left[\frac{1}{kPa^2}\right]$	167.1 $\left[\frac{1}{kPa}\right]$
4.4	0.645 $\left[\frac{\mu mol}{mg.s.kPa^2}\right]$	0.165 $\left[\frac{\mu mol}{mg.s.kPa^2}\right]$	1.187 $\left[\frac{1}{kPa^2}\right]$	36.53 $\left[\frac{1}{kPa}\right]$	-
4.5	0.918 $\left[\frac{\mu mol}{mg.s.kPa^2}\right]$	87.62 $\left[\frac{1}{kPa}\right]$	8.477 $\left[\frac{1}{kPa^2}\right]$	25.74 $\left[\frac{1}{kPa}\right]$	0.758 $\left[\frac{1}{kPa^2}\right]$
4.7	2.747 $\left[\frac{\mu mol}{mg.s.kPa^2}\right]$	0.245 $\left[\frac{\mu mol}{mg.s.kPa^2}\right]$	16.95 $\left[\frac{1}{kPa^2}\right]$	286.8 $\left[\frac{1}{kPa}\right]$	-
4.8	8.07×10^{-3} $\left[\frac{\mu mol}{mg.s.kPa}\right]$	0.021 $\left[\frac{1}{kPa}\right]$	-	-	-
4.12	0.0173 $\left[\frac{\mu mol}{mg.s.kPa^{0.83}}\right]$	-	-	-	-

Table 4.12. The kinetic parameters calculated in the model equations in the absence of H_2O and CO_2 at 110°C

	Kinetic Parameters				
Model Eqn.	K1	K2	K3	K4	K5
4.3	2.291 $\left[\frac{\mu mol}{mg.s.kPa^2}\right]$	0.355 $\left[\frac{\mu mol}{mg.s.kPa^2}\right]$	0.36 $\left[\frac{\mu mol}{mg.s.kPa^2}\right]$	12.69 $\left[\frac{1}{kPa^2}\right]$	154.05 $\left[\frac{1}{kPa}\right]$
4.4	0.719 $\left[\frac{\mu mol}{mg.s.kPa^2}\right]$	0.189 $\left[\frac{\mu mol}{mg.s.kPa^2}\right]$	2.5 $\left[\frac{1}{kPa^2}\right]$	24.77 $\left[\frac{1}{kPa}\right]$	-
4.5	0.743 $\left[\frac{\mu mol}{mg.s.kPa^2}\right]$	49.96 $\left[\frac{1}{kPa}\right]$	3.852 $\left[\frac{1}{kPa^2}\right]$	22.02 $\left[\frac{1}{kPa}\right]$	0.478 $\left[\frac{1}{kPa^2}\right]$
4.7	3.162 $\left[\frac{\mu mol}{mg.s.kPa^2}\right]$	0.497 $\left[\frac{\mu mol}{mg.s.kPa^2}\right]$	18.24 $\left[\frac{1}{kPa^2}\right]$	210.6 $\left[\frac{1}{kPa}\right]$	-
4.8	0.0107 $\left[\frac{\mu mol}{mg.s.kPa}\right]$	1.3×10^{-3} $\left[\frac{1}{kPa}\right]$	-	-	-
4.12	0.0232 $\left[\frac{\mu mol}{mg.s.kPa^{0.83}}\right]$	-	-	-	-

Table 4.13. The kinetic parameters calculated in the model equations in the absence of H_2O and CO_2 at 130°C

	Kinetic Parameters				
Model Eqn.	K1	K2	K3	K4	K5
4.3	1.724 $\left[\frac{\mu mol}{mg.s.kPa^2}\right]$	0.337 $\left[\frac{\mu mol}{mg.s.kPa^2}\right]$	0.338 $\left[\frac{\mu mol}{mg.s.kPa^2}\right]$	19.94 $\left[\frac{1}{kPa^2}\right]$	105.5 $\left[\frac{1}{kPa}\right]$
4.4	0.638 $\left[\frac{\mu mol}{mg.s.kPa^2}\right]$	0.212 $\left[\frac{\mu mol}{mg.s.kPa^2}\right]$	2 $\left[\frac{1}{kPa^2}\right]$	23.47 $\left[\frac{1}{kPa}\right]$	-
4.5	0.877 $\left[\frac{\mu mol}{mg.s.kPa^2}\right]$	58.5 $\left[\frac{1}{kPa}\right]$	8.575 $\left[\frac{1}{kPa^2}\right]$	33.52 $\left[\frac{1}{kPa}\right]$	10^{-5} $\left[\frac{1}{kPa^2}\right]$
4.7	2.194 $\left[\frac{\mu mol}{mg.s.kPa^2}\right]$	0.373 $\left[\frac{\mu mol}{mg.s.kPa^2}\right]$	20.99 $\left[\frac{1}{kPa^2}\right]$	149.3 $\left[\frac{1}{kPa}\right]$	-
4.8	9.56×10^{-3} $\left[\frac{\mu mol}{mg.s.kPa}\right]$	6.54×10^{-3} $\left[\frac{1}{kPa}\right]$	-	-	-
4.12	0.02 $\left[\frac{\mu mol}{mg.s.kPa^{0.83}}\right]$	-	-	-	-

The experimental results were also fit to the power law model in the absence of H_2O and CO_2, given in Equation (4.12), and the orders of α_{CO}=-0.07 and α_{O2}=0.9 were calculated with the R^2 of 0.98.

$$-r_{CO} = kP_{CO}^{-0.07} P_{O_2}^{0.9} \tag{4.12}$$

4.4.2. Parameter Estimation in the Presence of H_2O and CO_2

The kinetic parameters estimated in Equation (4.3), (4.4), (4.5), (4.7), (4.8) and (4.13) are given in Table 4.14., Table 4.15. and Table 4.16. in the presence of 10% H_2O and 25% CO_2 at 90°C, 110°C and 130°C. According to the results, the combined kinetic parameters calculated in the absence of H_2O and CO_2 have smaller values than that in the presence of 10% H_2O and 25% CO_2 at each temperature, i.e. 90°C, 110°C and 130°C.

Table 4.14. The kinetic parameters calculated in the model equations in the presence of 10% H_2O and 25% CO_2 at 90°C

	Kinetic Parameters				
Model Eqn.	K1	K2	K3	K4	K5
4.3	6.7 $\left[\frac{\mu mol}{mg.s.kPa^2}\right]$	0.7 $\left[\frac{\mu mol}{mg.s.kPa^2}\right]$	0.69 $\left[\frac{\mu mol}{mg.s.kPa^2}\right]$	1636.9 $\left[\frac{1}{kPa^2}\right]$	886.6 $\left[\frac{1}{kPa}\right]$
4.4	2.025 $\left[\frac{\mu mol}{mg.s.kPa^2}\right]$	0.372 $\left[\frac{\mu mol}{mg.s.kPa^2}\right]$	241.9 $\left[\frac{1}{kPa^2}\right]$	156.7 $\left[\frac{1}{kPa}\right]$	-
4.5	0.926 $\left[\frac{\mu mol}{mg.s.kPa^2}\right]$	176.8 $\left[\frac{1}{kPa}\right]$	215.3 $\left[\frac{1}{kPa^2}\right]$	8.506 $\left[\frac{1}{kPa}\right]$	52.2 $\left[\frac{1}{kPa^2}\right]$
4.7	5.2 $\left[\frac{\mu mol}{mg.s.kPa^2}\right]$	0.5 $\left[\frac{\mu mol}{mg.s.kPa^2}\right]$	1270.3 $\left[\frac{1}{kPa^2}\right]$	824.8 $\left[\frac{1}{kPa}\right]$	-
4.8	5.92×10^{-3} $\left[\frac{\mu mol}{mg.s.kPa}\right]$	1.8 $\left[\frac{1}{kPa}\right]$	-	-	-
4.13	0.004 $\left[\frac{\mu mol}{mg.s.kPa^{0.84}}\right]$	-	-	-	-

Table 4.15. The kinetic parameters calculated in the model equations in the presence of 10% H_2O and 25% CO_2 at 110°C

	Kinetic Parameters				
Model Eqn.	K1	K2	K3	K4	K5
4.3	5.886 $\left[\frac{\mu mol}{mg.s.kPa^2}\right]$	0.67 $\left[\frac{\mu mol}{mg.s.kPa^2}\right]$	0.68 $\left[\frac{\mu mol}{mg.s.kPa^2}\right]$	287.6 $\left[\frac{1}{kPa^2}\right]$	856 $\left[\frac{1}{kPa}\right]$
4.4	1.713 $\left[\frac{\mu mol}{mg.s.kPa^2}\right]$	0.384 $\left[\frac{\mu mol}{mg.s.kPa^2}\right]$	44.81 $\left[\frac{1}{kPa^2}\right]$	117.6 $\left[\frac{1}{kPa}\right]$	-
4.5	0.888 $\left[\frac{\mu mol}{mg.s.kPa^2}\right]$	97.8 $\left[\frac{1}{kPa}\right]$	52.12 $\left[\frac{1}{kPa^2}\right]$	48.05 $\left[\frac{1}{kPa}\right]$	26.95 $\left[\frac{1}{kPa^2}\right]$
4.7	5.964 $\left[\frac{\mu mol}{mg.s.kPa^2}\right]$	0.68 $\left[\frac{\mu mol}{mg.s.kPa^2}\right]$	292.5 $\left[\frac{1}{kPa^2}\right]$	865.5 $\left[\frac{1}{kPa}\right]$	-
4.8	4.57×10^{-3} $\left[\frac{\mu mol}{mg.s.kPa}\right]$	0.051 $\left[\frac{1}{kPa}\right]$	-	-	-
4.13	0.0072 $\left[\frac{\mu mol}{mg.s.kPa^{0.84}}\right]$	-	-	-	-

Table 4.16. The kinetic parameters calculated in the model equations in the presence of 10% H_2O and 25% CO_2 at 130°C

	Kinetic Parameters				
Model Eqn.	K1	K2	K3	K4	K5
4.3	7.2 $\left[\frac{\mu mol}{mg.s.kPa^2}\right]$	0.5 $\left[\frac{\mu mol}{mg.s.kPa^2}\right]$	0.51 $\left[\frac{\mu mol}{mg.s.kPa^2}\right]$	269.5 $\left[\frac{1}{kPa^2}\right]$	1094.1 $\left[\frac{1}{kPa}\right]$
4.4	3.752 $\left[\frac{\mu mol}{mg.s.kPa^2}\right]$	0.416 $\left[\frac{\mu mol}{mg.s.kPa^2}\right]$	61.48 $\left[\frac{1}{kPa^2}\right]$	307.57 $\left[\frac{1}{kPa}\right]$	-
4.5	1.014 $\left[\frac{\mu mol}{mg.s.kPa^2}\right]$	111.8 $\left[\frac{1}{kPa}\right]$	61.05 $\left[\frac{1}{kPa^2}\right]$	41.08 $\left[\frac{1}{kPa}\right]$	4.076 $\left[\frac{1}{kPa^2}\right]$
4.7	7.3 $\left[\frac{\mu mol}{mg.s.kPa^2}\right]$	0.5 $\left[\frac{\mu mol}{mg.s.kPa^2}\right]$	301.7 $\left[\frac{1}{kPa^2}\right]$	1064.1 $\left[\frac{1}{kPa}\right]$	-
4.8	4.7×10^{-3} $\left[\frac{\mu mol}{mg.s.kPa}\right]$	0.023 $\left[\frac{1}{kPa}\right]$	-	-	-
4.13	0.0091 $\left[\frac{\mu mol}{mg.s.kPa^{0.84}}\right]$	-	-	-	-

The power law model was also developed in the presence of H_2O and CO_2 (R^2=0.97) with the CO reaction order of α_{CO}=-0.06 and the O_2 reaction order of α_{O_2}=0.9 which are nearly the same as the values in the absence of H_2O and CO_2 supporting that the assumtion of the same mechanisms in both case may be valid.

$$-r_{CO} = kP_{CO}^{-0.06}P_{O_2}^{0.9} \tag{4.13}$$

4.4.3. Model Discrimination

Six models, i.e. Equation (4.3), (4.4), (4.5), (4.7), (4.8) and power law model showed a good fit between experimental and calculated data with high R^2 values. All possible mechanisms suggested the single-site model consistent with Langmuir-Hinselwood kinetics involving adsorption of CO and O_2 on the Au surface. The plots between

calculated rates using the parameters presented in previous sections and experimentally measured rates in the absence of H_2O and CO_2 are presented in Figure 4.7., whereas shown in Figure 4.8. in the presence of 10% H_2O and 25% CO_2.

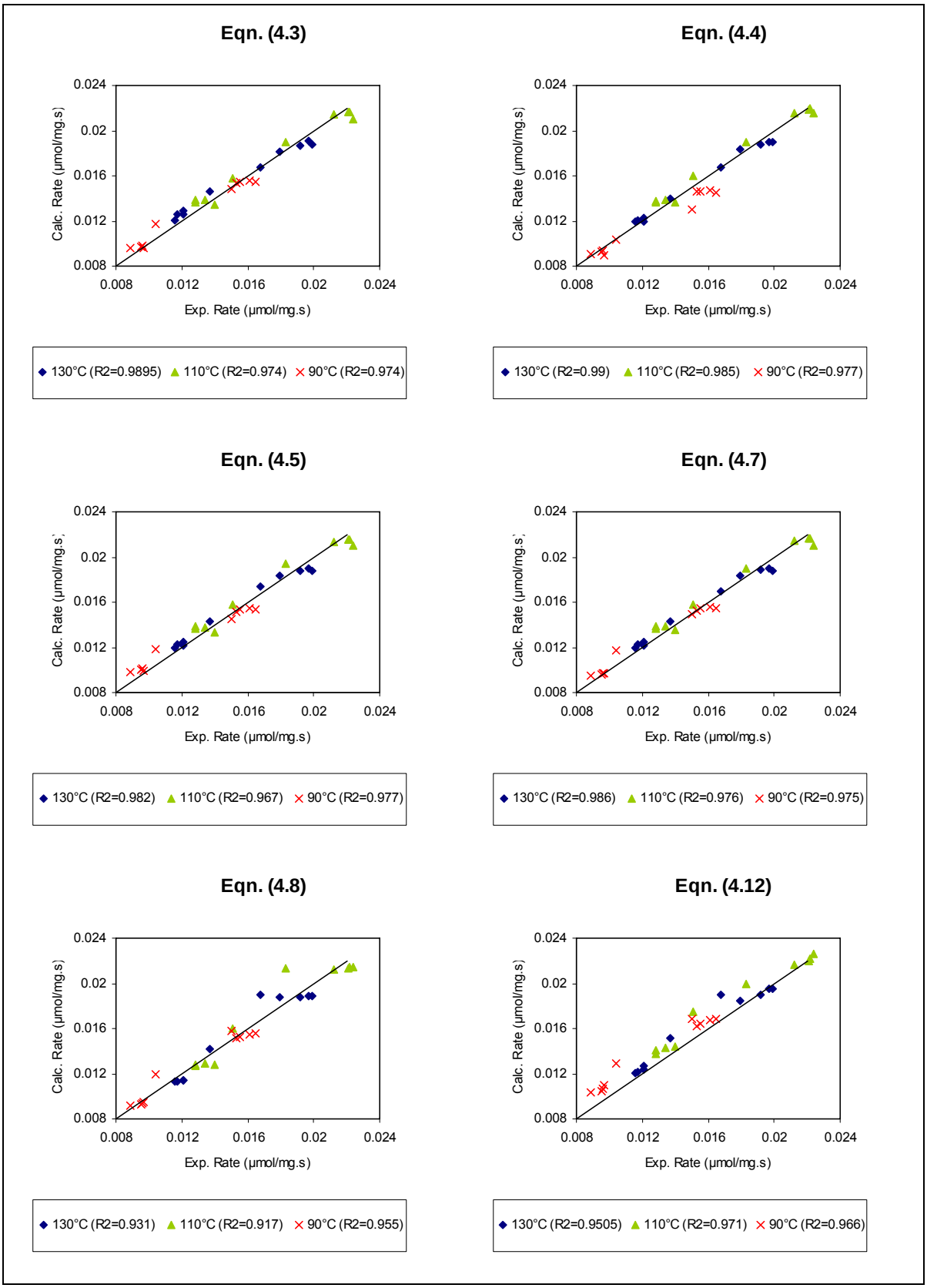

Figure 4.7. Calculated versus experimental rates in the absence of H_2O and CO_2

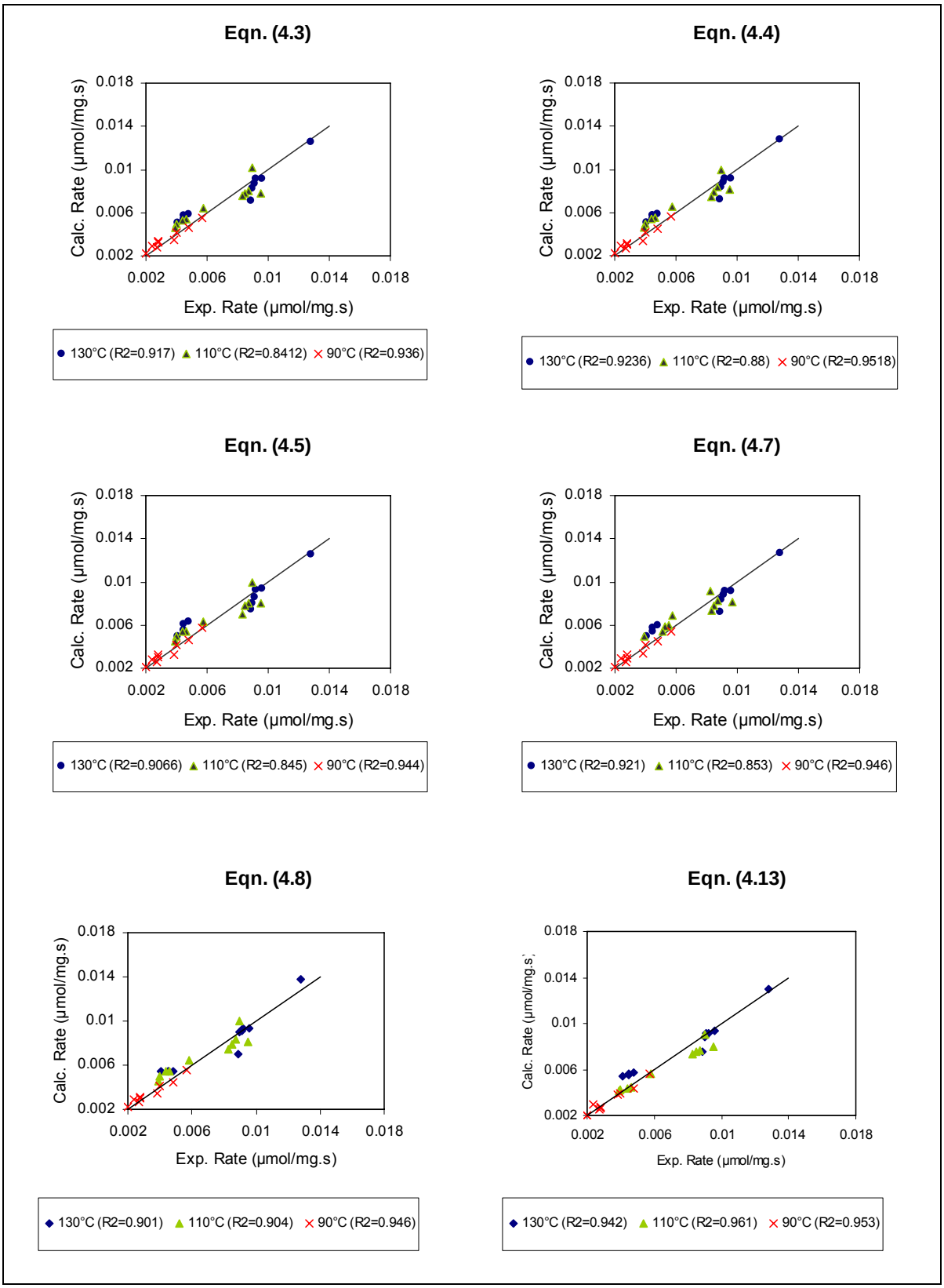

Figure 4.8. Calculated versus experimental rates in the presence of 10% H_2O and 25% CO_2

The six equations with high R^2 values were distinguished from the other four among the ten models proposed in Section 4.1., however no one of these six can be discriminated by looking the R^2 values. There were no discriminating difference between the results obtained in the absence and presence of H_2O and CO_2 either supporting the assumption that the presence of these two feed components affect only the rate parameters but not the mechanism.

On the other hand, the Equation (4.4) involving CO and O_2 adsorption on the Au surface or the Equation (4.5) with the formation of carbonate species ($-CO_3$) were seems to be more plausible. Although R^2 values of Equation (4.7) and (4.8) were also high, these were derived from a mechanism based on O_2 dissociation (Eqn. 4.6), which are turned out to be equivalent of Equation (4.4) containing no term about the dissociation due to the simplifying assumptions used. Since the performance of Equation (4.6) is weak and (4.7) and (4.8) contain no dissociative terms, we concluded that the dissociative mechanism is unlikely as it is commonly believed so unless an active support is used (Kung *et. al*., 2004); hence, we abondaned this mechanism and focused only on Equation (4.4) and (4.5).

It is generally known that the CO conversion in the absence of H_2 increases with increasing temperature, which is agreement with the study of Quinet *et. al*., (2008a). They studied the catalytic activity of gold-based catalysts in the absence and the presence of H_2. In the presence of H_2, the conversion increases first and then it starts to decreases with the further increase of the temperature, which exhibits similar behaviour to the work of Tezcanlı (2008). This may be attributed to the increasing H_2 adsorption with increasing temperature and blockage of the active sites available for CO oxidation. This is also observed in this study as evident from the change of CO conversion and rate as a function of temperature in Figure 4.9. and 4.10., respectively.

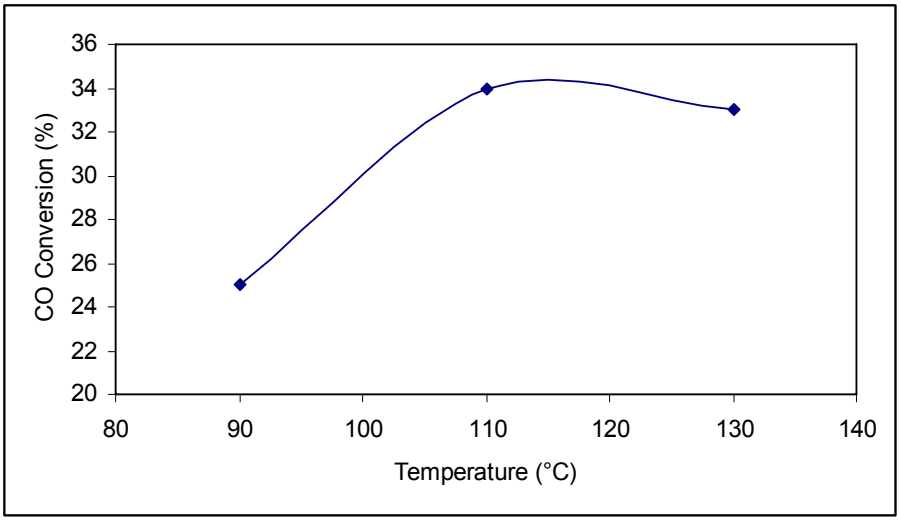

Figure 4.9. Temperature effects on CO conversion using 10 mg catalyst in the composition of 1% CO, 1% O_2, 60% H_2 and balance He

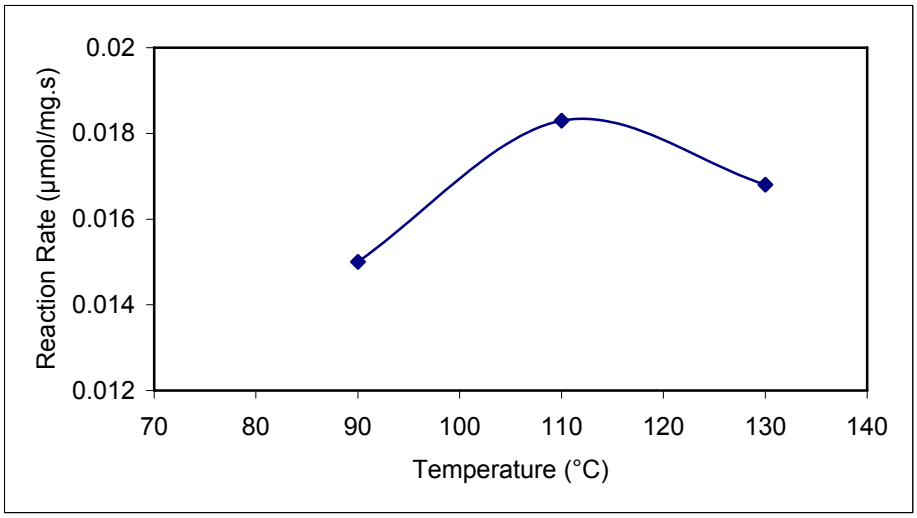

Figure 4.10. Temperature effects on reaction rate in the composition of 1% CO, 1% O_2, 60% H_2 and balance He

It is clear from Table 4.17. that CO adsorption term (K_1) in Equation (4.4) increases first and then it decreases again at 130^{o}C in the absence of H_2O and CO_2. k_2, which represents the O_2 adsorption on the other hand, increases continuosly supporting the argument that H_2 adsorption dominates at high temperatures. This is also evident from the fact that although CO conversion versus temperature plot exhibits a maximum, O_2 conversion continues to increase with increasing temperature. The same trend was observed for K_1 in Equation (4.5) (assuming that k_2 has the same values in both cases)

indicating that the CO/H_2 competition is indeed happening. k_3, representing the surface reaction term seems to have more than one reaction constant considering that it decreases first and then increases slightly. This may be also a further evidence for the effects of H_2 oxidation.

Table 4.17. The adsorption and reaction terms for Equation (4.4) and Equation (4.5) both in the absence and the presence of H_2O and CO_2

Parameter	Temperature	Condition			
		Equation (4.4)		Equation (4.5)	
		without H_2O and CO_2	with H_2O and CO_2	without H_2O and CO_2	with H_2O and CO_2
K_1	90°C	0.032	1.54	10.3	0.82
	110°C	0.1	0.38	12.9	1.87
	130°C	0.085	0.2	6.8	1.83
k_2	90°C	0.165	0.372	0.165	0.372
	110°C	0.189	0.384	0.189	0.384
	130°C	0.212	0.416	0.212	0.416
K_3	90°C	1141.8	101.8	-	-
	110°C	247.7	309.6	-	-
	130°C	276.1	1537.8	-	-
K_6	90°C	-	-	72.8	13.94
	110°C	-	-	50	57.5
	130°C	-	-	62.8	63.7
K_5	90°C	-	-	0.012	18.83
	110°C	-	-	0.006	0.58
	130°C	-	-	0.02	0.52

In the presence of CO_2 and H_2O, on the other hand, the CO conversion and oxidation rate increase with increasing temperature in the entire range indicating that H_2 effect is not significant (Figure 4.11. and 4.12.). This is an expected result since the presence of high concentration of H_2O suppresses the H_2 oxidation that is effective in the absence of water. This is also clear from that the equilibrium constant decreases with increasing temperature

in accordance with Le Chatelier's principle since the adsorption is exothermic. Similarly k_2 and k_3, also increase with increasing temperature. The other terms in the model are not conclusive at this stage.

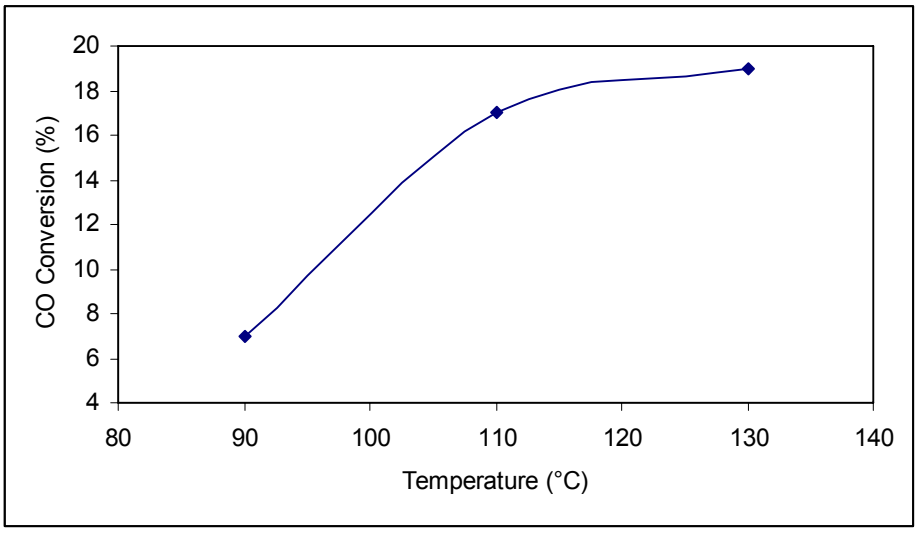

Figure 4.11. Temperature effects on CO conversion using 10 mg catalyst in the composition of 1% CO, 1% O_2, 10% H_2O, 25% CO_2, 60% H_2 and balance He

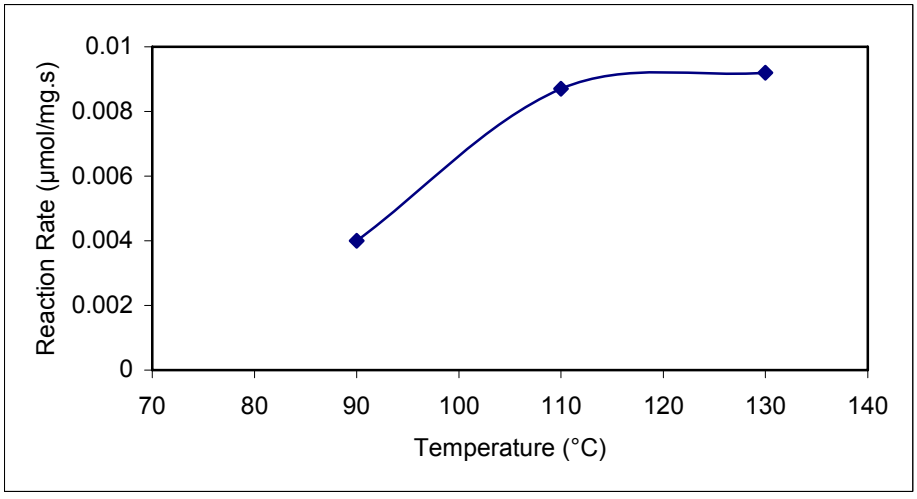

Figure 4.12. Temperature effects on reaction rate in the composition of 1% CO, 1% O_2, 10% H_2O, 25% CO_2, 60% H_2 and balance He

A similar trend was observed for K_1 calculated from Equation (4.5) in the absence of CO_2 and H_2O. However, in the presence of these two components, the behavior of K_1 does not seem to be in accordance with the experimental data, which require a decrease in K_1.

Considering that k_2 is assumed to be the same in both cases and the other terms in both equations are not conclusive, it can be conluded that Equation (4.4) seems to be more likely than Equation (4.5). However no definitive conclusion can be drawn at this stage because the unconclusive patterns in the equilibrium and the rate constants of Equation (4.5) may arises due to the fact that the reaction mechanism may be changing with the temperature as Haruta and Date (2001) suggested, and more than one mechanism may be valid in the temperature range studied

4.5. Effects of Temperature

In the absence of H_2O and CO_2, the CO conversion and the rate of CO consumption increased with increasing temperature 90°C to 110°C first and then decreases at 130°C, as presented in Figure 4.9. and 4.10. Tezcanlı (2008) studied the activity of Au/Al_2O_3 catalyst at temperature ranging 150°C to 50°C using feed composition of 1% CO, 1% O_2, 60% H_2, and 38% He. He was also concluded that the highest conversion was obtained at 60°C and CO conversion started to decline. The study by Rossignol *et. al*. (2005) in 2% CO, 2% O_2, 48% H_2, and balanced He is also consistent with our results, where decreasing temperature from 250°C to 119°C has positive effects on catalytic activity, whereas the activity decreased sharply from 119°C because of the competitional adsorption between CO and H_2. Although the temperature at which the maximum conversion varies from study to study due to the changing catalyst and reaction conditions, the trend is a general one and seems to be related to H_2 oxidation as discussed in previous section.

The effects of temperature on CO conversion and rate in the presence of H_2O and CO_2, on the other hand, is positive in the entire range (90^oC to 130^oC) studied as it presented in Figere 4.11. and 4.12. and explained by the fact that the H_2 oxidation may be prevented by the steam in the feed. The insignificance of H_2 oxidation for this case is also evident from the fact that the temperature dependent of k_3 calculated from Equation (4.4) exibits Arrhenius type behavior with a relatively high R^2 value of 0.92 (Figure 4.13.). The activation energy and the pre-exponential factor A were calculated as 71.1 $kJ.mol^{-1}$ and $2.2x10^{12}$ $\mu mol.mg^{-1}.s^{-1}.kPa^{-2}$, respectively. The drawing the Arrhenious plot was not possible in the absence of H_2O and CO_2 as a further evidence for the complications created by hydrogen.

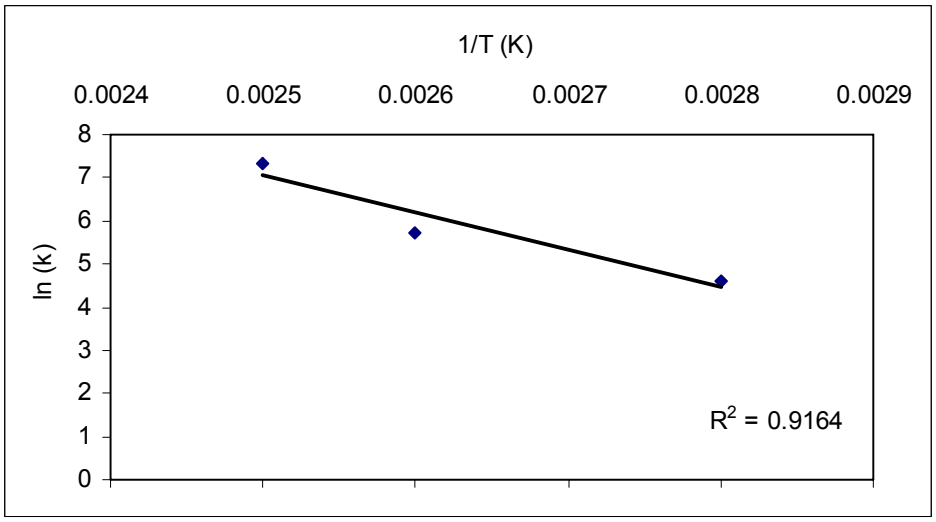

Figure 4.13. Arrhenius plot for Equation (4.4)
in the presence of 10% H_2O and 25% CO_2

The Arrhenius plot for k_6 in Equation (4.5) also produced a good statistical fitness with the R^2 of 0.93 supporting the discussion in the previous section that the mechanism may be still possible. The activation energy and preexponential factor for this case found to be 44.5 kJ.mol^{-1} and 4.9x10^7 μmol.mg^{-1}.s^{-1}.kPa^{-2}, respectively.

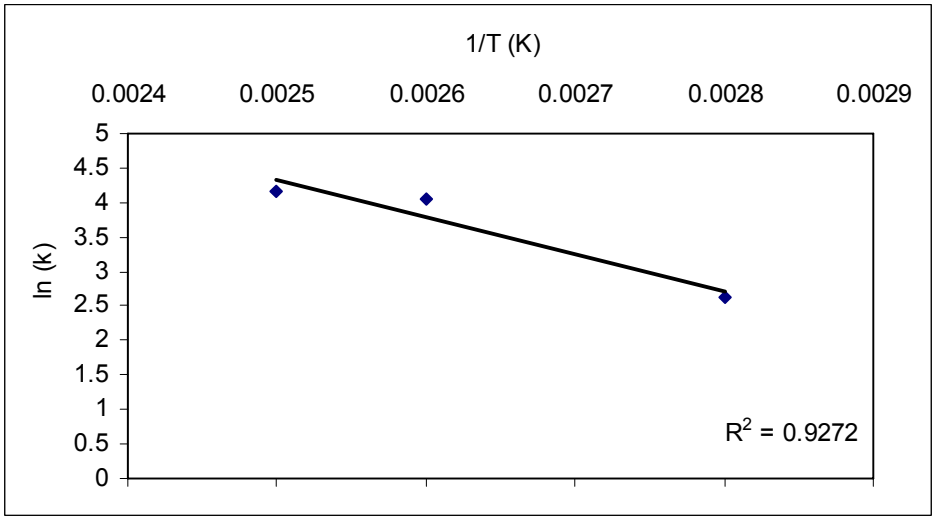

Figure 4.14. Arrhenius plot for Equation (4.5)
in the presence of H_2O and CO_2

The rate constant calculated from the power low model was also fitted to the Arrhenius plot. The fit was perfect with a R^2 value of almost 1 in the presence of 10% H_2O

and 25% CO_2 (Figure 4.15.). It was found that the apparent activation energy was 23 kJ.mol^{-1} and the pre-exponential factor A was 9.38 μmol.mg^{-1}.s^{-1}.Pa$^{-0.84}$. The fit in the absence of H_2O and CO_2 was weak again with an R^2 value of 0.6323.

The activation energy values calculated for Equation (4.4), Equation (4.5) and power law model were consistent with the activation energies reported for CO oxidation over supported gold catalysts, ranging from 1.5 to 74 kJ.mol^{-1}.

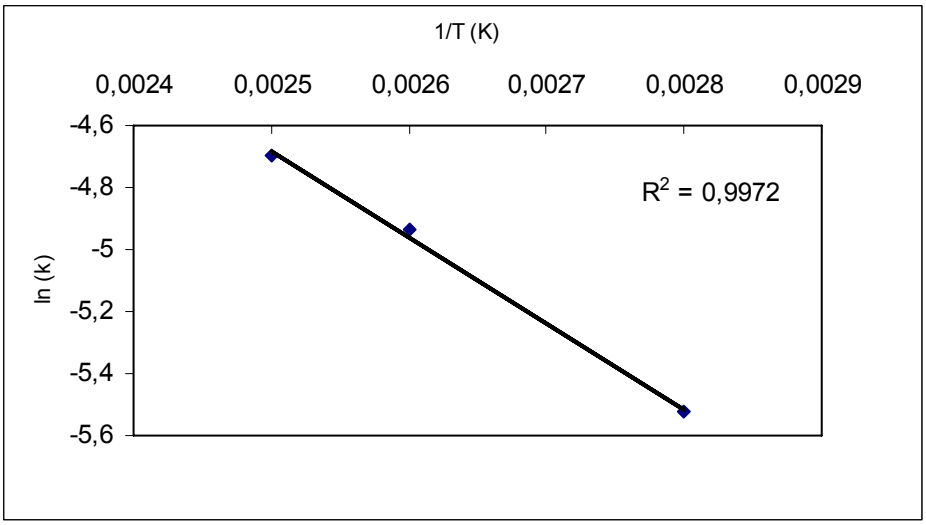

Figure 4.15. Arrhenius plot for power law model
in the presence of 10% H_2O and 25% CO_2

4.6. Catalyst Characterization

The amounts of Au loaded on 1% Au/Al_2O_3 and 0.5% Au/Al_2O_3 catalysts were measured by TUBİTAK using Inductively Coupled Plasma (ICP) and showed in Table 4.18.

Table 4.18. The results of Au loading

Catalyst	Measured Au loaded (wt%)
1% Au/Al_2O_3	0.93 %
0.5% Au/Al_2O_3	0.42 %

As illustrated in Table 4.18, Au contents in the two catalysts were very close to the nominal values, which made it possible to understand the Au effects on the catalytic activity.

5. CONCLUSIONS AND RECOMMENDATIONS

5.1. Conclusions

This study focused on the kinetic study of selective CO oxidation over Au/Al_2O_3 catalyst. The CO oxidation rates were evaluated using various concentrations of CO and O_2 at two residence times and three temperatures (90^oC, 110^oC and 130°C) for each concentration sets in differential model. The kinetic parameters in rate equations built from the mechanisms in the literature were calculated using non-linear least squares method coded in computer software MATLAB 7.4.0 (2007). The conclusions from this study were summarized as following;

- The same effects of CO and O_2 were observed on CO consumption rate both in the absence and the presence of 10 per cent H_2O and 25 per cent CO_2 but the addition of H_2O and CO_2 lowered rate values. CO consumption rate was negatively dependent on CO concentration, while positively on O_2 concentration.
- In order to reduce CO conversion for kinetic performance without H_2O and CO_2, 0.5 per cent Au of the Au/Al_2O_3 catalyst was selected. The decreasing Au content from 1 to 0.5 per cent negatively affected the catalytic activity, whereas no significant changes were observed between 0.5 and 0.3 per cent of Au. Decreasing temperature from 130 to 110°C exhibited positive effects on the activity of the catalyst, but CO conversion has decreased at 90°C.
- There was no significant difference between the performances of the six plausible models distibused among ten proposed. The mechanisms comprising the adsorption of O_2 and the adsorption of CO on the surface of Au and the mechanism involving the formation of CO_3 species exhibited a good fit between calculated data and experimentally measured data both in the absence and presence of H_2O and CO_2.
- The temperature dependence of CO oxidation rate is quite different in the absence and the presence of H_2O and CO_2 and this can be explained by the equilibrium and rate parameters in both model Equation (4.4) and (4.5) as an evidence of

plausibility of these two mechanism. It can be then concuded that the CO oxidation proceeds between adsorbed CO and O_2 but it is not clear whether an adsorbed CO_3 intermediate exist (Equation 4.5) or not (Equation 4.4)

- Equation (4.4), (4.5) and power law models were tested using Arrhenius plot between lnk vs. 1/T and activation energies found in the presence of H_2O and CO_2 were in agreement with the activation energies given in literature. This result can be considered as further evidence supporting the previous conclusion. After the measurement of the Au content, it was found that the amounts of Au in the catalysts were very close to nominal values.

5.2. Recommendations

Based on the results of the present study, the below recommendations can be helpful for the kinetic studies of CO oxidation on gold-based catalysts.

- The effects of H_2 on the kinetic analysis should be taken into account. Since H_2 oxidation can affect the mechanism of CO oxidation and cause the formation of H_2O, H_2 oxidation and CO oxidation may be investigated in the same study.
- FTIR measurements should be used to indicate whether Au catalyzes the formation of the intermediate species on the catalyst surface and the gas molecules in the feed or species are adsorbed on the surface sites, which can directly help the mechanism of CO on Au/Al_2O_3 be understood.
- Kinetic calculations of the present study may be repeated using the integral method with necessary experimental data in order to obtain the comparisons between differential and integral methods according to the model discrimination.

REFERENCES

Adachi, H., S. Ahmed, S. H. D. Lee, D. Papadias, R. K. Ahluwalia, J. C. Bendert, S. A. Kanner and Y. Yamazaki, 2009, "A Natural-Gas Fuel Processor for a Residential Fuel Cell System", *Journal of Power Sources*, Vol. 188, pp. 244-255.

Aguilar-Guerrero, V. and B. C. Gates, 2008, "Kinetics of CO Oxidation Catalyzed by Highly Dispersed CeO_2-Supported Gold", *Journal of Catalysis*, Vol. 260, pp. 351-357.

Alcaide, F., P. L. Cabot and E. Brillas, 2006, "Fuel Cells for Chemicals and Energy Cogeneration", *Journal of Power Sources*, Vol. 153, pp. 47-60.

Avcı, A. K., Z. İ. Önsan and D. L. Trimm, 2001, "On-board Fuel Conversion for Hydrogen Fuel Cells: Comparison of Different Fuels by Computer Simulations", *Applied Catalysis A: General*, Vol. 216, pp. 243-256.

Avgouropoulos, G., T. Ioannides, C. Papadopoulou, J. Batista, S. Hocevar and H. K. Matralis, 2002, "A Comparative Study of Pt/γ-Al_2O_3, Au/α-Fe_2O_3 and CuO-CeO_2 Catalysts for the Selective Oxidation of Carbon Monoxide in Excess Hydrogen", *Catalysis Today*, Vol. 75, pp. 157-167.

Azar, M., V. Caps, F. Morfin, J. L. Rousset, A. Piednoir, J. C. Bertolini and L. Piccolo, 2006, "Insights into Activation, Deactivation and Hydrogen-Induced Promotion of a Au/TiO_2 Reference Catalyst in CO Oxidation", *Journal of Catalysis*, Vol. 239, pp. 307-312.

Baltacıoğlu, F. S., B. Gülyüz, A. E. Aksoylu and Z. İ. Önsan, 2007, "Low Temperature CO Oxidation Kinetics over Activated Carbon Supported Pt-SnO_x Catalysts", *Turkish Journal of Chemistry*, Vol. 31, pp. 455-464.

Boccuzzi, F., A. Chiorino and M. Manzoli, 2001, "Au/TiO_2 Nanostructured Catalyst: Effects of Gold Particle Sizes on CO Oxidation at 90 K", *Materials Science and Engineering*, Vol. 15, pp. 215-217.

Boccuzzi, F., A. Chiorino and M. Manzoli, 2000, "FTIR Study of the Electronic Effects of CO Adsorbed on Gold Nanoparticles Supported on Titania", *Surface Science*, Vols. 454-456, pp. 942-946.

Bond, G. C., C. Louis and D. T. Thompson, 2006, *Catalysis by Gold,* Imperial College Press, England.

Bond, G. C. and D. T. Thompson, 2000, "Gold-Catalyzed Oxidation of Carbon Monoxide", *Gold Bulletin*, Vol. 33, pp. 41-51.

Caputo, T., L. Lisi, R. Pirone and G. Russo, 2008, "On the Role of Redox Properties of CuO/CeO_2 Catalysts in the Preferential Oxidation of CO in H_2-rich Gases", *Applied Catalysis A: General*, Vol. 348, pp. 42-53

Centeno, M. A., K. Hadjiivanov, T. Venkov, H. Klimev and J. A. Odriozola, 2006, "Comparative Study of Au/Al_2O_3 and Au/CeO_2-Al_2O_3 Catalysts", *Journal of Molecular Catalysis A: Chemical*, Vol. 252, pp. 142-149.

Chang, C. T., B. J. Liaw, Y. P. Chen and Y. Z. Chen, 2009, "Characteristics of Au/Mg_xAlO Hydrotalcite Catalysts in CO Selective Oxidation", *Journal of Molecular Catalysis A: Chemical*, Vol. 300, pp. 80-88.

Chang, L. H., N. Sasirekha, B. Rajesh and Y. W. Chen, 2007, "CO Oxidation on Ceria- and Manganese Oxide-Supported Gold Catalysts", *Separation and Purification Technology*, Vol. 58, pp. 211-218.

Chen, Y. Z., B. J. Liaw, J. M. Wang and C. T. Huang, 2008, "Selective Removal of CO from Hydrogen-Rich Stream over $CuO/Ce_xSn_xO_2$-Al_2O_3 Catalysts", *International Journal of Hydrogen Energy*, Vol. 33, pp. 2389-2399.

Costello, C. K., J. H. Yang, H. Y. Law, Y. Wang, J. N. Lin, L. D. Marks, M. C. Kung and H. H. Kung, 2003, "On the Potential Role of Hydroxyl Group in CO Oxidation over Au/Al_2O_3", *Applied Catalysis A: General*, Vol. 243, pp. 15-24.

Daniells, S. T., A. R. Overweg, M. Makkee and J. A. Moulijn, 2005, "Mechanism of Low-Temperature CO Oxidation with Au/Fe_2O_3 Catalyst: A Combined Mössbauer, FT-IR, and TAP Reactor Study", *Journal of Catalysis*, Vol. 230, pp. 52-65.

Dandan-Candan, T., A. E. Aksoylu and R. Yıldırım, 2009, "Reaction Pathway Analysis for CO Oxidation over Anionic Gold Hexamers Using DFT", *Journal of Molecular Catalysis A: Chemical*, Vol. 306, pp. 118-122.

Date, M., H. Imai, S. Tsubota and M. Haruta, 2007, "In Situ Measurements under Flow Condition of the CO Oxidation over Supported Gold Nanoparticles", *Catalysis Today*, Vol. 122, pp. 222-225.

Ersoz, A., H. Olgun and S. Ozdogan, 2006, "Simulation Study of a Proton Exchange Membrane (PEM) Fuel Cell System with Autothermal Reforming", *Energy*, Vol. 31, pp. 1490-1500.

Fogler, H. S., 2006, *Elements of Chemical Reaction Engineering*, Prentice-Hall, Englewood Cliffs, New Jersey.

Froment, G. F. and K. B. Bischoff, 1990, *Chemical Reactor Analysis and Design,* Wiley, New York.

Gavril, D., A. Georgaka, V. Loukopoulos and G. Karaiskakis, 2007, "Gas Chromatographic Investigation of the Effects of Hydrogen and Temperature on the

Nature of the Active Sites Related to CO Adsorption on Nanosized Au/γ-Al_2O_3", *Journal of Chromatography A*, Vol. 1164, pp. 271-280.

Georgaka, A., D. Gavril, V. Loukopoulos, G. Karaiskakis and B. E. Nieuwenhuys, 2008, "H_2 and CO_2 Coadsorption Effects in CO Adsorption over Nanosized Au/γ-Al_2O_3 Catalysts", *Journal of Chromatography*, Vol. 1205, pp. 128-136.

Ghenciu, A. F., 2002, "Review of Fuel Processing Catalysts for Hydrogen Production in PEM Fuel Cells Systems", *Current Opinion in Solid State and Materials Science*, Vol. 6, pp. 389-399.

Gottfried, J. M. and K. Christmann, 2004, "Oxidation of Carbon Monoxide over Au (110)–(1x2)", *Surface Science*.

Grisel, R. J. H., C. J. Westrate, A. Goossens, M. W. J. Craje, A. M. van der Kraan and B. E. Nieuwenhuys, 2002, "Oxidation of CO over Au/MO_x/Al_2O_3 Multi-Component Catalysts in a Hydrogen-Rich Environment", *Catalysis Today*, Vol. 72, pp. 123-132.

Grisel, R. J. H. and B. E. Nieuwenhuys, 2001a, "A Comparative Study of the Oxidation of CO and CH_4 over Au/MO_x/Al_2O_3 Catalysts", *Catalysis Today*, Vol. 64, pp. 69-81.

Grisel, R. J. H. and B. E. Nieuwenhuys, 2001b, "Selective Oxidation of CO over Supported Au Catalysts", *Journal of Catalysis*, Vol. 199, pp. 48-59.

Gurbani, A., J. L. Ayastuy, M. P. Gonzalez-Marcos, J. E. Herrero, J. M. Guil and M. A. Gutierrez-Ortiz, 2009, "Comparative Study of CuO-CeO_2 Catalysts Prepared by Wet Impregnation and Deposition-Precipitation", *International Journal of Hydrogen Energy*, Vol. 34, pp. 547-553.

Günay, M. E. and R. Yıldırım, 2008, "Neural Network Aided Design of Pt-Co-Ce/Al_2O_3 Catalyst for Selective CO Oxidation in Hydrogen-rich Streams", *Chemical Engineering Journal*, Vol. 140, pp. 324-331.

Haruta, M., 2004, "Nanoparticulate Gold Catalysts for Low-Temperature CO Oxidation", *Journal of New Materials for Electrochemical Systems*, Vol. 7, pp. 163-172.

Haruta, M. and M. Date, 2001, "Advances in the Catalysis of Au Nanoparticles", *Applied Catalysis A: General*, Vol. 222, pp. 427-437.

Haruta, M., S. Tsubota, T. Kobayashi, H. Kageyama, M. J. Genet and B. Delmon, 1993, "Low Temperature Oxidation of CO over Gold Supported on TiO_2, α-Fe_2O_3 and Co_3O_4", *Journal of Catalysis*, Vol. 144, pp. 175-192.

Haryanto, A., S. Fernando and S. Adhikari, 2007, "Ultrahigh Temperature Water Gas Shift Catalysts to Increase Hydrogen Yield from Biomass Gasification", *Catalysis Today*, Vol. 129, pp. 269-274.

Hoebink, J. H. B. J., J. M. A. Harmsen, M. Balenovic, A. C. P. M. Backx and J. C. Schouten, 2001, "Automotive Exhaust Gas Conversion from Elementary Step Kinetics to Prediction of Emission Dynamics", *Topics in Catalysis*, Vol. 16/17, pp. 319-327.

Holladay, J.D., J. Hu, D. L. King and Y. Wang, 2009, "An Overview of Hydrogen Production Technologies", *Catalysis Today*, Vol. 139, pp. 244-260.

Holladay, J., E. Jones, D. R. Palo, M. Phels, Y. H. Chin, R. Dagle, J. Hu, Y. Wang and E. Baker, 2004, "Miniature Fuel Processors for Portable Fuel Cell Power Supplies", *Materials Research Society Symposium Proceedings*, Vol. 756.

Hvolbaek, B., T. V. W. Janssens, B. S. Clausen, H. Falsig, C. H. Christensen and J. K. Norskov, 2007, "Catalytic Activity of Au Nanoparticles", *Nanotoday*, Vol. 2, pp. 14-18.

Hwang, S. M., O. J. Kwon, S. H. Ahn and J. J. Kim, 2009, "Silicon-Based Micro-reactor for Preferential CO Oxidation", *Chemical Engineering Journal*, Vol. 146, pp. 105-111.

Iizuka, Y., T. Miyamae, T. Miura, M. Okumura, M. Date and M. Haruta, 2009, "A Kinetic Study on the Low Temperature Oxidation of CO over Ag-Contaminated Au Fine Powder", *Journal of Catalysis*, Vol. 262, pp. 280-286.

İnce, T., G. Uysal, A. N. Akın and R. Yıldırım, 2005, "Selective Low-Temperature CO Oxidation over Pt-Co-Ce/Al_2O_3 in Hydrogen-rich Streams", *Applied Catalysis A: General*, Vol. 292, pp. 171-176.

Ivanova, S., V. Pitchon and C. Petit, 2006a, "Application of the Direct Exchange Method in the Preparation of Gold Catalysts Supported on Different Oxide Materials", *Journal of Molecular Catalysis A: Chemical*, Vol. 256, pp. 278-283.

Ivanova, S., V. Pitchon, Y. Zimmermann and C. Petit, 2006b, "Preparation of Alumina Supported Gold Catalysts: Influence of Washing Procedures, Mechanism of Particles Size Growth", *Applied Catalysis A: General*, Vol. 298, pp. 57-64.

Jayasankar, B. R., A. Ben-Zvi and B. Huang, 2009, "Identifiability and Estimability Study for a Dynamic Solid Oxide Fuel Cell Model", *Computers and Chemical Engineering*, Vol. 33, pp. 484-492.

Khoudiakov, M., M. C. Gupta and S. Deevi, 2005, "Au/Fe_2O_3 Nanocatalysts for CO Oxidation: A Comparative Study of Deposition-Precipitation and Coprecipitation Techniques", *Applied Catalysis A: General*, Vol. 291, pp. 151-161.

Kim, D. H. and M. S. Lim, 2002, "Kinetics of Selective CO Oxidation in Hydrogen-rich Mixtures on Pt/Alumina Catalysts", *Applied Catalysis A: General*, Vol. 224, pp. 27-38.

Kung, M. C., C. K. Costello and H. H. Kung, 2004, "CO Oxidation over Supported Au Catalysts", *Catalysis*, Vol.17, pp.152-165.

Kung, H. H., M. C. Kung and C. K. Costello, 2003, "Supported Au Catalysts for Loe Temperature CO Oxidation", *Journal of Catalysis*, Vol.216, pp.425-432.

Lai, X., D. Liu, L. Peng and J. Ni, 2008, "A Mechanical-Electrical Finite Element Method Model for Predicting Contact Resistance between Bipolar Plate and Gas Diffusion Layer in PEM Fuel Cells", *Journal of Power Sources*, Vol.182, pp.153-159.

Lai, X., T. P .S. Clair, M. Valden and D. W. Goodman, 1998, "Scanning Tunneling Microscopy Studies of Metal Clusters Supported on TiO_2 (110): Morphology and Electronic Structure", *Progress in Surface Science*, Vol. 59, pp. 25-52.

Lee, H. S., A. Ray, O. Lane and J. E. McGrath, 2008, "Synthesis and Characterization of Poly(arylene Ether Sulfone)-bypolybenzimidazole Copolymers for High Temperature Low Humidity Proton Exchange Membrane Fuel Cells", *Polymer,* Vol. 49, pp. 5387-5396.

Lee, S. J. and A. Gavriilidis, 2002, "Supported Au Catalysts for Low-Temperature CO Oxidation Prepared by Impregnation", *Journal of Catalysis,* Vol. 206, pp. 305-313.

Leppelt, R., B. Schumacher, V. Plzak, M. Kinne and R. J. Behm, 2006, "Kinetics and Mechanism of the Low-Temperature Water-Gas Shift Reaction on Au/CeO_2 Catalysts in an Idealized Reaction Atmosphere", *Journal of Catalysis,* Vol.244, pp. 137-152.

Li, M., D.H. Wang, X. C. Shi, Z. T. Zhang, T. X. Dong, 2007, "Kinetics of Catalytic Oxidation of CO over Copper-Manganese Oxide Catalyst", *Separation and PurificationTechnology,* Vol. 57, pp. 147-151.

Liu, B. and Y. Zhang, 2008, "Status and Prospects of Intermediate Temperature Solid Oxide Fuel Cells", *Journal of University of Science and Technology Beijing,* Vol. 15, pp. 84.

Liu, Z. P., P. Hu and A. Alavi, 2002, "Catalytic Role of Gold in Gold-Based Catalysts; A Density Functional Theory Study on the CO Oxidation on Gold", *Journal of The American Chemical Society,* Vol. 124, pp. 14770-14779.

Long, C. G., J. D. Gilbertson, G: Vijayaraghavan, K. J. Stevenson, C. J. Pursell and B. D. Chandler, 2008, "Kinetic Evaluation of highly Active Supported Gold Catalysts Prepared from Monolayer-Protected Clusters: An Experimental Michaelis-Menten Approach for Determining the Oxygen Binding Constant during CO Oxidation Catalysis", *Journal of The American Chemical Society,* Vol. 130, pp.10103-10115.

Lopez, N., T. V. W. Janssens, B. S. Clausen, Y. X. M. Mavrikakis, T. Bligaard and J. K. Norskov, 2004, "On the Origin of the Catalytic Activity of Gold Nanoparticles for Low-Temperature CO Oxidation", *Journal of Catalysis,* Vol. 223, pp. 232-235.

Luengnaruemitchai, A., S. Osuwan and E. Gulari, 2004, "Selective Catalytic Oxidation of CO in the Presence of H_2 over Gold Catalyst", *International Journal of Hydrogen Energy,* Vol. 29, pp. 429-435.

Manzoli, M., A. Chiorino and F. Boccuzzi, 2003, "FTIR Study of Nanosized Gold on ZrO_2 and TiO_2", *Surface Science,* Vols. 532-535, pp. 377-382.

Martinez-Arias, A., A. B. Hungria, G. Munuera and D. Gamarra, 2006, "Preferential Oxidation of CO in Rich H_2 over CuO/CeO_2: Details of Selectivity and Deactivation under the Reactant Stream", *Applied Catalysis B: Environmental,* Vol. 65, pp. 207-216.

Masel, R. I., 2001, *Chemical Kinetics and Catalysis,* Wiley-Interscience, New York.

MATLAB, Version 7.4.0, The MathWorks Inc., 2007.

Mazer, T. S., D. A. Dziuba, C. T. P. Vieira and F. B. Passos, 2009, "The Effect of Copper on the Selective Carbon Monoxide Oxidation over Alumina Supported Gold Catalysts", *Journal of Powe ,* Vol. 187, pp. 209-215.

Menegazzo, F., F. Pinna, M. Signoretto, V. Trevisan, F. Boccuzzi, A. Chiorino and M. Manzoli, 2009, "Quantative Determination of Sites Able to Chemisorb CO on Au/ZrO_2 Catalysts", *Applied Catalysis A: General,* Vol. 356, pp. 31-35.

Mhadeshwar, A. B. and D. G. Vlachos, 2005, "Hierarchial Multiscale Surface Reaction Mechanism Development: CO and H_2 Oxidation, Water-Gas Shift, and Preferential Oxidation of CO on Rh", *Journal of Catalysis,* Vol. 234, pp. 48-63.

Mozer, T. S., D. A. Dziuba, C. T. P. Vieira and F. B. Passos, 2009, "The Effect of Copper on the Selective Carbon Monoxide Oxidation over Alumina Supported Gold Catalysts", *Journal of Power Sources,* Vol. 187, pp. 209-215.

Natesakhawat, S., X. Wang, L. Zhang and U. S. Ozkan, 2006, "Development of Chromium-Free Iron-Based Catalysts for High-Temperature Water-Gas Shift Reaction", *Journal of Molecular Catalysis A: Chemical,* Vol. 260, pp. 82-94.

Oliva, D. G., J. A. Francesconi, M. C. Mussati and P. A. Aguirre, 2008, "CO-PROX Reactor Design by Model-Based Optimization", *Journal of Power Sources,* Vol. 182, pp. 307-316.

Önsan, Z. İ., 2007, "Catalytic Processes for Clean Hydrogen Production from Hydrocarbons", *Turkish Jouırnal of Chemistry,* Vol. 31, pp. 531-550.

Özyönüm, G. N., A. N. Akın and R. Yıldırım, 2007, "Kinetic Study of Selective CO Oxidation over Pt-Co-Ce/Al_2O_3 Catalyst in Hydrogen-Rich Streams", *Turkish Journal of Chemistry,* Vol. 31, pp. 445-453.

Pansare, S. S., A. Sirijaruphan and J. G. J. Goodwin, 2005, "Au-Catalyzed Selective Oxidation of CO: A Steady State Isotopic Transient Kinetic Study", *Journal of Catalysis,* Vol. 234, pp. 151-160.

Park, E. D., D. Lee and H. C. Lee, 2009, "Recent Progress in Selective CO Removal in a H_2-Rich Stream", *Catalysis Today,* Vol. 139, pp. 280-290.

Pradhan, S., A. S. Reddy, R. N. Devi and S. Chilukuri, 2009, "Copper-Based Catalysts for Water Gas Shift Reaction; Influence of Support on Their Catalytic Activity", *Catalysis Today,* Vol. 141, pp. 72-76.

Prestianni, A., A. Martorana, F. Labat, I. Ciofini and C. Adamo, 2009, "A DFT Investigation of CO Oxidation over Neutral and Cationic Gold Clusters", *Journal of Molecular Structure: THEOCHEM,* Vol. 903, pp. 34-40.

Quinet, E., F. Morfin, F. Diehl, P. Avenier, V. Caps and J. L. Rousset, 2008a, "Hydrogen Effect on the Preferential Oxidation of Carbon Monoxide over Alumina-Supported Gold Nanoparticles", *Applied Catalysis B: Environmental,* Vol. 80, pp. 195-201.

Quinet, E., L. Piccolo, H. Daly, F.C. Meunier, F. Morfin, A. Valcarcel, F. Diehl, P. Avenier, V. Caps and J. L. Rousset, 2008b, "H_2-Induced Promotion of CO Oxidation over Unsupported Gold", *Catalysis Today,* Vol. 138, pp. 43-49.

Rabenstein, G. and V. Hacker, 2008, "Hydrogen for Fuel Cells from Ethanol by Steam-Reforming, Partial Oxidation and Combined Autothermal Reforming: A Thermodynamic Analysis", *Journal of Power Sources,* Vol. 185, pp. 1293-1304.

Ribeiro, N. F. P., F. M. T. Mendes, C. A. C. Perez, M. M. V. M. Souza and M. Schmal, 2008, "Selective CO Oxidation with Nano Gold Particles-Based Catalysts over Al_2O_3 and ZrO_2", *Applied Catalysis A: General,* Vol. 347, pp. 62-71.

Rossignol, C., S. Avrii, F. Morfin, L. Piccolo, V. Caps and J. L. Rousset, 2005, "Selective Oxidation of CO over Model Gold-Based Catalysts in the Presence of H_2", *Journal of Catalysis,* Vol. 230, pp. 476-483.

Romero-Sarria, F., A. Penkova, L. M. Martinez, T. M. A. Centeno, K. Hadjiivanov and J. A. Odriozola, 2008, "Role of Water in the CO Oxidation Reaction on Au/CeO_2; Modification of the Surface Properties", *Applied Catalysis B: Environmental,* Vol. 84, pp. 119-124.

Sandoval, A., A. Gomez-Cortes, R. Zanella, G. Diaz and J. M. Saniger, 2007, "Gold Nanoparticles; Support Effects for the WGS Reaction", *Journal of Molecular Catalysis A: Chemical,* Vol. 278, pp. 200-208.

Schmal, M., M. M. V. M. Souza, N. S. Resende, A. L. Guimaraes, C. A. Perez, J. G. Eon, D. A. G. Aranda and L. C. Dieguez, 2005, "Interpretation of Kinetic Data with Selected Characterizations of Active Sites", *Catalysis Todal,* Vol. 100, pp. 145-150.

Schubert, M. M., A. Venugopal, M. J. Kahlich, V. Plzak and R. J. Behm, 2004, "Influence of H_2O and CO_2 on the Selective CO Oxidation in H_2-Rich Gases over $Au/\alpha\text{-}Fe_2O_3$", *Journal of Catalysis,* Vol. 222, pp. 32-40.

Seitarides, T., C. Athanasiou and A. Zabaniotou, 2008, "Modular Biomass Gasification-Based Solid Oxide Fuel Cells (SOFC) for Sustainable Development", *Renewable and Sustainable Energy Reviews,* Vol. 12, pp. 1251-1276.

Soares, J. M. C., P. Morrall, A. Crossley, P. Harris and M. Bowker, 2003, "Catalytic and Noncatalytic CO Oxidation on Au/TiO_2 Catalysts", *Journal of Catalysis,* Vol. 219, pp. 17-24.

Son, I. H., M. Shamsuzzoha and A. M. Lane, 2002, "Promotion of $Pt/\gamma\text{-}Al_2O_3$ by New Pretreatment for Low-Temperature Preferential Oxidation of CO in H_2 for PEM Fuel Cells", *Journal of Catalysis,* Vol. 210, pp. 460-465.

Song, C., 2002, "Fuel Processing for Low-Temperature and High-Temperature Fuel Cells Challenges, and Opportunities for Sustainable Development in the 21st Century", *Catalysis Today,* Vol. 77, pp. 17-49.

Souza, M. M. V. M., N. F. P. Ribeiro and M. Schmal, 2007, "Influence of the Support in Selective CO Oxidation on Pt Catalysts for Fuel Cell Applications", *International Journal of Hydrogen Energy,* Vol. 32, pp. 425-429.

Szabo, E. G., A. Tompos, M. Hegedus, A. Szegedi and J. Margitfalvi, 2007, "The Influence of Cooling Atmosphere after Reduction on the Catalytic Properties of Au/Al_2O_3 and Au/MgO Catalysts in CO Oxidation", *Applied Catalysis A: General,* Vol. 320, pp. 114-121.

Tezcanlı, S. T.,2008, *Au-based Catalyst Design for Selective CO Oxidation in Hydrogen-Rich Streams*, M. S. Thesis, Boğaziçi University, Istanbul.

Trimm, D. L., 2005, "Minimisation of Carbon Monoxide in a Hydrogen Stream for Fuel Cell Application", *Applied Catalysis A: General,* Vol. 296, pp. 1-11.

Trimm, D. L. and Z. İ. Önsan, 2001, "Onboard Fuel Conversion for Hydrogen-Fuel-Cell-Driven Vehicles", *Catalysis Reviews,* Vol. 43 (1&2), pp. 31-84.

Tseng, C. H., T. C. K. Yang and H. E. Wu, 2008, "Catalysis of Oxidation of Carbon Monoxide on Supported Gold Nanoparticle", *Journal of Hazardous Materials.*

Venkoz, T., H. Klimev, M. A. Centeno, J. A. Odriozola and K. Hadjiivanov, 2006, "State of Gold on an Au/Al_2O_3 Catalyst Subjected to Different Pre-treatments: An FTIR Study", *Catalysis Communications,* Vol. 7, pp. 308-313.

Wen, L., J. K. Fu, P. Y. Gu, B. X. Yao, Z. H. Lin and J. Z. Zhou, 2008, "Monodispersed Gold Nanoparticles Supported on γ-Al_2O_3 for Enchancement of Low- Temperature Catalytic Oxidation of CO", *Applied Catalysis B: Environmental,* Vol. 79, pp. 402-409.

Wojciechowski, B. W and N. M. Rice, 2003, *Experimental Methods in Kinetic Studies,* Elsevier, Boston.

Wojciechowski, B. W. and S. P. Asprey, 2000, "Kinetic Studies Using Temperature-Scanning: The Oxidation of Carbon Monoxide", *Applied Catalysis A: General,* Vol. 190, pp. 1-24.

Yang, Y., X. Du, L. Yang, Y. Huang and H. Xian, 2009, "Investigation of Methane Steam Reforming in Planar Porous Support of Solid Oxide Fuel Cell", *Applied Thermal Engineering,* Vol. 29, pp. 1106-1113.

Yu, L., G. Ren, M. Qin and X. Jiang, 2009, "Transport Mechanisms and Performance Simulations of a PEM Fuel Cell with Interdigitated Flow Field", *Renewable Energy,* Vol. 34, pp. 530-543.

Yu, W.Y., W. S. Lee, C. P. Yang and B. Z. Wan, 2007, "Low-Temperature Preferential Oxidation of CO in a Hydrogen Rich Stream (PROX) over Au/TiO_2: Thermodynamic Study and Effect of Gold-Colloid pH Adjustment Time on Catalytic Activity", *Journal of the Chinese Institute of Chemical Engineers,* Vol. 38, pp. 151-160.

Zou, X., S. Qi, Z. Suo, L. An and F. Li, 2007, "Activity and Deactivation of Au/Al_2O_3 Catalyst for Low-Temperature CO Oxidation", *Catalysis Communications,* Vol. 8, pp. 784-788.